ELSEVIER

Journal of Chromatography A, 971 (2002) 1–35

JOURNAL OF CHROMATOGRAPHY A

www.elsevier.com/locate/chroma

Review

Laser-based non-fluorescence detection techniques for liquid separation systems

T. de Beer*, N.H. Velthorst, U.A.Th. Brinkman, C. Gooijer

Department of Analytical Chemistry and Applied Spectroscopy, Vrije Universiteit Amsterdam, De Boelelaan 1083, 1081 HV Amsterdam, The Netherlands

Received 5 March 2002; received in revised form 10 July 2002; accepted 11 July 2002

Abstract

Over the last two decades, the possibility to use lasers for detection purposes in column liquid chromatography (LC) and capillary electrophoresis (CE) received much attention in the analytical chemistry literature. Most attention has been devoted to laser-induced fluorescence. The present review covers developments on non-fluorescence techniques for LC and CE. The techniques considered are thermal lens spectrometry, photoacoustic detection, refractive index detection including refractive index backscattering, Raman spectroscopy and degenerate four-wave mixing (a special mode of transient holographic spectroscopy). The paper starts with an outline of the characteristics of lasers; it ends with an overall evaluation and a discussion of the perspectives of the techniques dealt with.

Keywords: Reviews; Detection, LC; Detection, CE; Laser-based non-fluorescence detection

Contents

*Corresponding author.
E-mail address: tjipke.debeer@spark.nl (T. de Beer).

0021-9673/02/$ – see front matter
PII: S0021-9673(02)01038-5

1. Introduction

Over the last two decades, the possibility to use lasers in detection systems that can be combined with liquid separation techniques such as column liquid chromatography (LC) and capillary electrophoresis (CE) received much attention in the analytical chemistry literature. This can be readily understood in view of the trend to miniaturize separation systems and make detection volumes extremely small. Most attention has been devoted to laser-induced fluorescence (LIF), which is a quite attractive method in view of the extremely favourable limits of detection (LODs), both in terms of concentration units and of injected mass and is without doubt the most utilized laser-based detection technique. However, LIF-based detection also has some disadvantages. Firstly, in most instances chemical derivatization has to be used to enable the application of LIF, either because the analytes do not exhibit native fluorescence or because they cannot be excited at the available laser wavelengths. It should be realized that for analytes requiring fluorogenic or fluorescent labelling, in practice it is the chemistry and not the LIF detection itself that determines the LODs that can be achieved. In fact, chemical derivatization of analytes in complex matrices cannot be applied at 10^{-8}–10^{-9} M analyte levels in real-life samples. Here, one may refer to the papers of Kwakman et al. [1,2] and Mank and co-workers [2–9]. Fortunately, the second problem encountered in the past when trying to excite natively fluorescent analytes in the UV region, is no longer a serious one since various laser types emitting in this wavelength region have become commercially available in the last couple of years. An additional advantage of analysing the non-derivatized compound is that on-line recording of fluorescence emission spectra can be used for tentative identification purposes, as has been extensively discussed in a recent review paper [10].

The present review covers developments on laser-based non-fluorescence detection techniques for LC and CE; LIF is not included since it received much attention in the recent literature. Techniques to be discussed and evaluated are: thermal lens spectrometry, photoacoustic detection, refractive index detection including refractive index backscattering, Raman spectroscopy and degenerate four-wave mixing (which can be considered as a special mode of transient holographic spectroscopy). Detection techniques in which the laser is, in essence, used for sample handling purposes, such as matrix-assisted laser desorption ionisation time-of-flight mass spectrometry (MALDI–TOF-MS), are not considered. Evaporative light scattering detection (ELSD) is not included either; commercial ELSD systems are already available and, furthermore, in general ELSD is a lamp-based instead of a laser-based technique. It should be added that thermal lens spectrometry,

photoacoustic detection and degenerate four-wave mixing are all based on heat generation upon (laser) light absorption; that is, in principle, they reflect the absorption characteristics of the analyte. On the other hand, with refractive index detection where absorption of light is avoided, the main parameter is the analyte mole fraction.

Most of the above techniques are exclusively used for detection purposes; they have no identification power. In this review, they will be evaluated by using conventional (lamp-based) absorption detection as the reference technique. The only, favourable, exception is Raman spectroscopy. It is based on inelastic light scattering and provides vibrational characteristics of the analyte molecule. In fact, it is receiving wide attention in the recent literature because of its identification power. Before considering the various techniques, a brief discussion will be devoted to the characteristics of laser instrumentation.

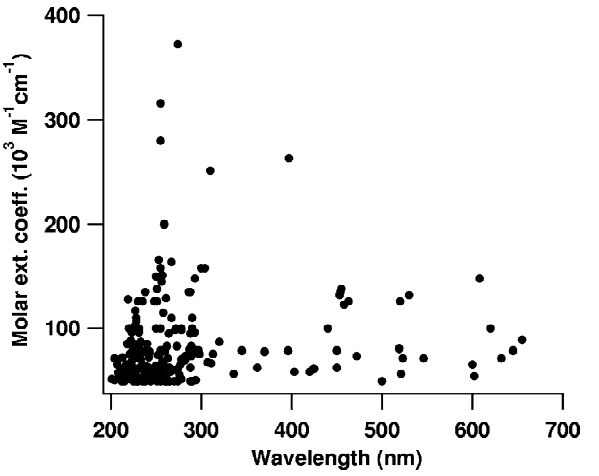

Fig. 1. Molar extinction coefficients versus wavelength for 300 organic compounds. Data from [14].

2. Characteristics of lasers

2.1. History

After the discovery of the laser by Maiman in 1960 [11–13], some time elapsed before analytical chemists recognized its potential. Before 1980, laser systems were usually bulky instruments which consumed much electrical energy (>25 kW) and cooling water (>1 m^3/h). Furthermore, they required high investment and maintenance costs. Usually only a few discrete wavelengths (longer than 300 nm) were available. In addition, skilled technicians were needed to operate the lasers. Consequently, a laser was not the first choice for an analytical chemist. The preferred light source in detection systems should allow fast and easy wavelength scanning and, besides, deliver radiation in the UV part of the electromagnetic spectrum, where most analytes have their maximum extinction coefficient (see Fig. 1) [14]. On the other hand, lasers provide a powerful, directional beam that can ultimately be focused to a spot with a diameter close to the wavelength concerned (typically 1 μm); they deliver a high spectral radiance (amount of power in a certain wavelength interval) and, finally, their radiation is coherent. These unique features make a laser an ideal instrument for detection purposes in micro-bore LC (μLC) and CE [15]. In Fig. 2, the wavelengths and the output power of several popular lasers in analytical chemistry are visualised.

Progress in laser and optical development eliminated a large part of the disadvantages. For instance (intracavity) harmonic generation (i.e., doubling, tripling or even quadrupling the frequency of the output) and frequency-up conversion (where the output of two lasers is summed to a new frequency) yield a wider range of attractive wavelengths, including UV output [16]. Both techniques use a so-called

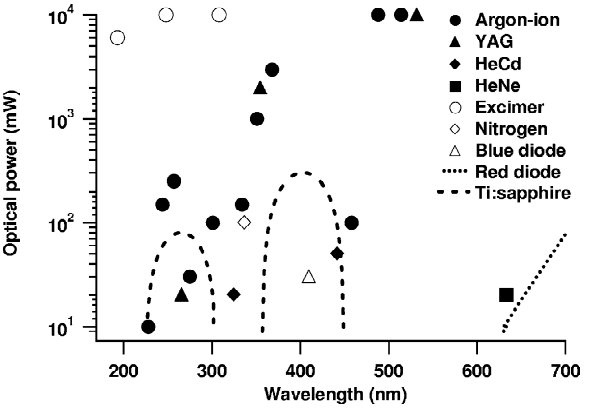

Fig. 2. Output power and wavelengths of various laser systems including intracavity frequency-doubled lasers.

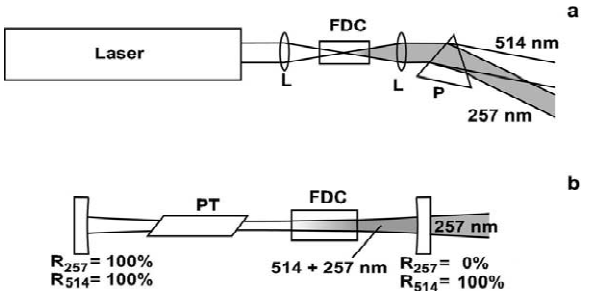

Fig. 3. Second harmonic generation set-ups (a) outside and (b) inside the laser cavity (intracavity frequency doubling). Abbreviations: FDC, frequency doubling crystal; L, focusing lenses; P, prism; PT, laser plasma tube. R_{514} and R_{257} indicate the reflection coefficients for the mirrors at 514 and 257 nm, respectively.

non-linear crystal (a specially cut crystal of $LiNbO_3$ or $NH_4H_2PO_4$) to convert the visible laser radiation to the UV, as shown in Fig. 3. In Fig. 3a, a frequency-doubling set-up using an argon-ion laser is shown. Such a set-up provides a conversion efficiency of about 1% when using an optical power of 0.5 W of 514 nm [17], but it should be noted that the conversion ratio is strongly dependent on the laser power used. Inside the laser cavity, the optical power is much higher (500 W or even more) so that placing the non-linear crystal in the laser cavity is very favourable. By using a dichroic mirror which reflects the fundamental radiation and transmits the frequency-doubled light, all the available power of the laser can be provided as UV light, as shown in Fig. 3b. Such a development is the intracavity frequency-doubled argon-ion laser, that emits some lines in the deep UV (the most important ones being 257, 244 and 229 nm). These are turnkey systems which have already been commercialized.

The new small-size, quadrupled Nd:YAG lasers deserve attention as well. These lasers deliver a few mW average power of 266 nm radiation at a repetition rate as high as about 8 kHz in sub-nanosecond pulses. These compact devices are inexpensive and robust, with lifetimes of 10 000 h. Such lasers will be of high interest in CE of bioanalytical samples since the excitation wavelength matches the fluorescence excitation maxima of the natively fluorescent amino acids tyrosine, tryptophan and phenylalanine [18,19].

Furthermore, Ti:sapphire lasers will contribute to the further exploration of new fields in analytical spectroscopy. Combined with frequency-doubling or -tripling techniques, these lasers provide a tunability range from about 230 to 310 nm and from about 350 to 460 nm, as indicated in Fig. 2. Their repetition rate up to 100 MHz and pulse durations on the (sub-)picosecond level will open new possibilities for detection in analytical separation systems [20,21]. Their widespread use in Raman-based detection can be anticipated [22–24]. In addition, one may expect that semiconductor lasers (diode lasers) emitting in the green, blue or even in the UV region of the electromagnetic spectrum will be introduced within the next few years [25]. Actually, a diode laser emitting at wavelengths around 410 nm has already been commercialized [26].

Finally, it should be emphasized that modern lasers are easy to operate. Therefore, it can be safely stated that at present lasers are promising instruments for analytical chemists. It should be noted, however, that state-of-the-art lasers are mainly used in LIF-based detection techniques. Most of the techniques to be discussed in this overview still use standard, more or less traditional, laser systems.

2.2. Pulsed lasers

There are two main types of lasers: continuous-wave (CW) and pulsed lasers. Pulsed lasers used in analytical laboratories over the last 10–15 years typically deliver their optical output as short intense pulses, usually about 10 ns wide, at a repetition rate of 100 Hz. The peak power during a pulse is extremely high—tens of megawatts is no exception. Pulsed lasers such as excimer and nitrogen lasers use an electrical discharge to excite the gas in a tube while solid-state lasers such as the Nd:YAG laser are usually pumped with a flash lamp. Advantages of pulsed lasers are the high peak powers that can be generated without using cooling water and high-power lines, so that frequency doubling, tripling and/or quadrupling the laser output (to obtain shorter wavelengths) can be easily utilized. Excimer lasers can deliver mid- and deep UV radiation at an average power level of about 10 W (cf. Fig. 2). Furthermore, the short pulse allows time-gated detection if the induced signal is still present after the exciting laser pulse has died out.

Of course, there are also some inherent drawbacks. Due to the high peak power, saturation and analyte degradation may occur, which limit the sensitivity and linearity of the detection method. The duty cycle is low (typically 10^{-6}), which implies that for pulsed laser systems which do not have a high peak power (as holds for the quadrupled Nd:YAG lasers with a low repetition rate), there is simply not enough optical power to perform sensitive measurements. The pulse-to-pulse repeatability is usually poor (typically 10%) and is a serious source of noise. For improved performance, averaging over many pulses is required, as can be seen in Fig. 4: for a laser with a repetition rate of 100 Hz an averaging time of 1 s leads to a 10-fold reduction of noise, i.e., to 1%. Unfortunately, the averaging time is limited. It should not exceed the detector response time usually applied in (μ)LC and CE in order to prevent band broadening. Fig. 4 shows that the effect of averaging is most prominent for narrow peaks, that is, averaging of pulses has to be done very carefully in micro-separation systems.

2.3. Continuous-wave lasers

CW lasers emit their output continuously, and intensity is constant over time. Some CW lasers provide only low power, e.g., a few mW. Nonetheless, because of the high directionality of the laser output, even for such lasers the spectral irradiance is usually high enough for various detection purposes. The noise level of a CW laser is typically 0.5%—a figure that can be compared to the pulse-to-pulse repeatability of pulsed lasers, since both describe the output stability over a certain period of time—and even can be improved down to 0.01% by using stabilizing techniques controlled by feedback. Other advantages of CW over pulsed lasers are the higher beam quality (which is almost perfectly Gaussian) and the high degree of coherence (for instance, HeNe lasers provide coherence lengths of typically 30 m). On the other hand, CW lasers that provide UV output are still rare.

Some CW lasers can be used in a quasi-pulsed mode by means of, e.g., mode-locking: the laser is operated in the CW mode, but by inserting intracavity elements a pulsed output is obtained [27]. Mode-locked lasers essentially provide the combined advantages of CW and pulsed lasers—a stable output together with a high peak power—and furthermore a high repetition rate of about 100 MHz. The high peak power is advantageous for frequency—doubling the output of the laser to the UV. The high repetition rate enables efficient averaging of the signals. The above-mentioned Ti:sapphire laser is based on this technique.

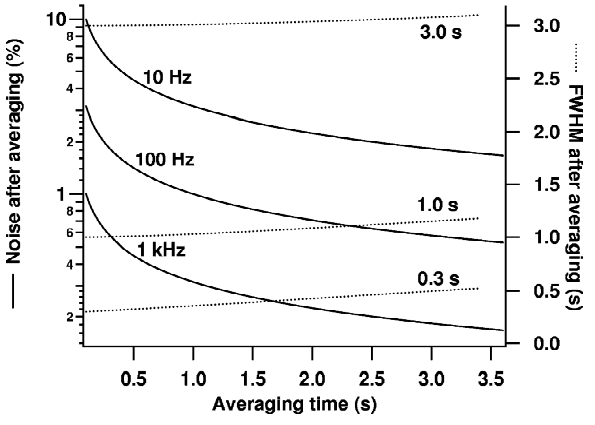

Fig. 4. Effect of averaging of laser pulses. The solid lines represent the noise remaining after averaging, and the dashed curves the influence of the averaging time on the width of a chromatographic peak.

2.4. Diode lasers

Diode lasers, which are based on semiconductor technology, deserve particular attention. They are rather inexpensive (down to US$ 25) and can be battery operated since they need a current of only a few mA. Due to their small size, a detector based on a diode laser can be extremely compact, which is ideal for micro-separation systems [28,29]. Major disadvantages are the relatively long emission wavelengths (until recently not shorter than 670 nm) and the relatively low power provided (tens of mW). The best-known example is the GaAlAs laser that emits near-IR radiation at 780 nm and is the workhorse of the compact-disk industry. Due to the demand for compact optical information storage and broadband telecommunication (glass-fibre) links, there is a rapid development in this field and significant progress has been achieved in recent years [30–32]. For instance, inexpensive InGaAlP lasers that emit in the visible

range of the electromagnetic spectrum have become commercially available. These lasers provide 10 mW at 670 nm and 3 mW at 635 nm.

Diode lasers can replace the pump source in solid-state lasers as well, thereby reducing the overall system size and costs. For instance, diode-laser pumped intracavity frequency-doubled Nd:YAG lasers providing 5 mW of 532 nm radiation can be operated on a battery and are sold for less than US$ 1000. The total package, including the Nd:YAG rod, the frequency-doubling optics and the (3 V Li^+) battery, has the dimensions of only an ordinary laser pointer.

Shorter wavelengths from diode lasers can be obtained by using frequency-doubling. Unfortunately, frequency-doubling is inefficient at the low input powers that are provided by diode lasers. Depending on the conditions (such as doubling-crystal type and length), a conversion ratio of 1×10^{-6} to 4×10^{-4} can be obtained, which results in several tens of μWs in the blue wavelength region (420–445 nm) [33]. Much research is devoted to improve the frequency-doubling materials; encouraging conversion ratios of 0.1 have been achieved. Higher conversion ratios can also be attained by making use of intracavity frequency-doubling but, unfortunately, such systems are less robust [33].

Recently, a violet-emitting laser diode, based on GaN (gallium nitride), became commercially available [26]. The diode operates at a fixed wavelength between 390 and 420 nm with a power of 5 mW (although short operations up to 10 mW are allowed); the lifetime has been estimated at 2000–5000 h. LIF applications using this new device have already been reported; however, a derivatization step was necessary or LIF was used in the indirect mode [34,35]. Evidently, exciting native fluorescence is still rare at these wavelengths.

2.5. Lasers in micro-separation systems

As already noted, lasers provide a powerful, directional and coherent beam that can be focused into a small—typically 0.1–1 nl—volume, and are therefore ideal for detection purposes in μLC and CE. Furthermore, with these light sources, detection schemes can be designed that were previously difficult to implement because conventional light sources provide too low spectral irradiances and incoherent radiation. This especially applies for Raman spectroscopy, refractive index backscattering and degenerate four-wave mixing, as will be outlined below.

At this point, an important aspect of laser-based detection should be noted. The LODs that can be achieved are of course related to the signal-to-noise (S/N) ratio. However, increasing the optical power does not always result in a better detection performance. For linear detection techniques, such as LIF, photo-acoustic and Raman spectroscopy, both S and N are proportional to the optical power under flicker-noise conditions—a problem which is directly related to the stability of the used laser—and, consequently, the overall S/N is not improved. This has been visualized in Fig. 5a, where S/N remains essentially the same over a large power interval. Contrary to the linear detection techniques, for non-linear ones such as four-wave mixing detection, higher powers are favourable (viz. Fig. 5b). It should be realized that there are limitations to the laser

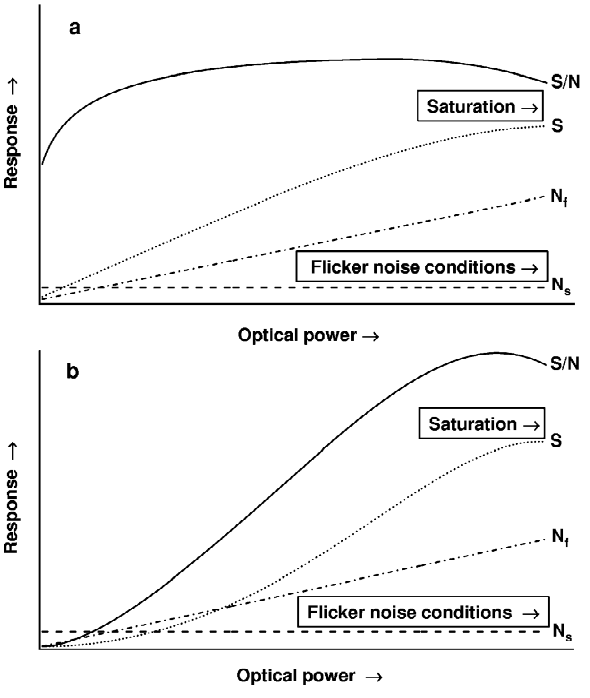

Fig. 5. Signal (S), flicker-noise (N_f), shot-noise (N_s) and S/N (where $N=N_f+N_s$) as a function of optical power for (a) linear and (b) non-linear detection techniques.

power that can be used: at too high optical power levels, saturation effects play a role and photodestruction of analyte molecules becomes more prominent [36,37], and S/N decreases (see Fig. 5). Furthermore, such deteriorated signals usually prohibit proper quantitation and should therefore be prevented. The point where saturation or photodestruction effects will show up cannot easily be predicted. It depends on the wavelength of the laser radiation, the photostability of the analyte and on experimental conditions such as the focal lengths of the lenses, the solvents used and their flow-rates.

As already noted, the preferred wavelengths in most detection techniques are located in the UV part of the electromagnetic spectrum (cf. Fig. 1). Currently available (CW) lasers are the helium:cadmium (HeCd) laser, which emits radiation at 325 nm, and the argon-ion laser that has some lines in the mid-UV (around 350 nm). Under special conditions output at shorter wavelengths is provided by large-frame argon-ion lasers, the most important one being the 275 nm line [38] (cf. Fig. 2). Recently, commercially intracavity frequency-doubled argon-ion and krypton-ion lasers were introduced, which emit lines as short as 229 nm. Unfortunately, such systems are still rather expensive. It can be expected that the recently introduced quadrupled Nd:YAG lasers, that provide 266-nm radiation, will become widely applied [18,19]. At present, the most applications of all these lasers are concerned with LIF detection.

3. Thermal lens spectrometry

Thermal lens spectrometry (TLS) is a thermo-optical technique based on the temperature rise within a sample upon absorption of light [39]. Radiation is absorbed by (the chromophoric group of) the analyte molecules, which are excited and subsequently lose their energy by a radiative (fluorescence or phosphorescence) or a non-radiative (vibrational relaxation via collisions with the immediately surrounding solvent molecules) route. Even if the analyte molecule follows a radiative pathway after being excited, some heat will still be generated due to the Franck–Condon effect and vibrational relaxation processes to reach the equilibrated vibrational ground state of the S_1 and the S_0 electronic states, respectively. Since the refractive index (RI) of the solvent changes with temperature, the heated sample solution shows local RI disturbances, which deflects the incoming radiation or alters the propagation of a second, so-called probe beam (pump-probe TLS).

The first observation of a thermal lens generated in this way was reported by Gordon et al. [40]. They observed undesired lensing effects during a Raman study of pure liquids when inserting the sample cell inside the cavity—which was done to take advantage of the high intracavity laser power—of a HeNe laser. The induced thermal lens degraded the laser oscillation and thus increased the radiation losses since much radiation was defocused outside the laser cavity. Furthermore, the mode structure of the output deteriorated, which is the main reason why intracavity thermal lensing should be avoided. Therefore, TLS measurements are performed outside the cavity. A schematic showing single-beam, double-beam (see Section 3.1) and pump-probe TLS is given in Fig. 6a–c, respectively. In order to achieve sufficient irradiance to induce thermal lensing, a lens is used to focus the laser beam into the sample that is positioned beyond the focal plane of the lens. After transmission through the sample, the beam passes a diaphragm and strikes a photodetector. The induced increase of the divergence of the beam caused by the thermal lens is detected by measuring the reduction of light intensity, since after the defocusing process part of the beam is blocked by the diaphragm. In a pump-probe set-up, the defocusing step applies for the probe beam as well.

In the last decade, TLS was reviewed by various workers active in this field [41–45]. Quite recently, TLS applications were reviewed by Franko [46]. In this paper, we confine ourselves to the application of TLS as a detection technique for (micro-) separation systems.

3.1. Theoretical aspects

In order to evaluate the performance of TLS, the signals generated in absorption spectrometry and TLS are compared. In conventional absorption spectrometry, the transmitted signal is given by Lambert–Beer's law:

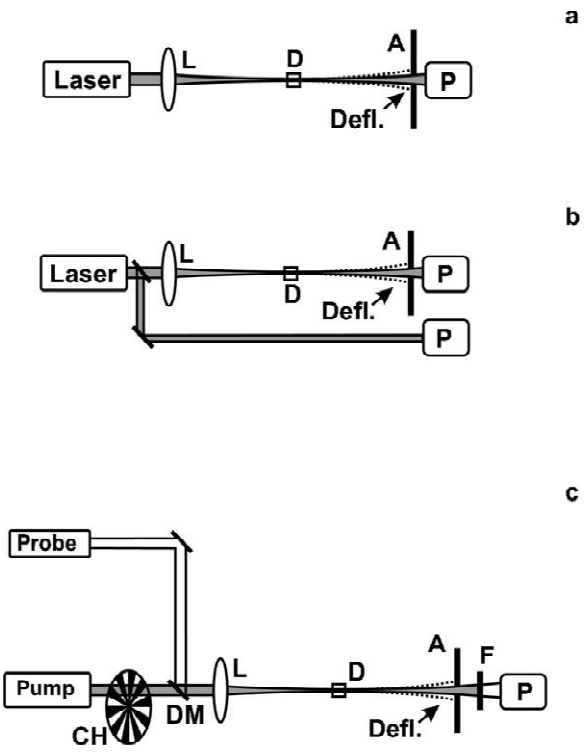

Fig. 6. Schematic of TLS detection set-ups. (a) single-beam; (b) double-beam; (c) pump-probe. Abbreviations: L, focusing lens; D, detector cell; P, photodiode; HeNe, helium:neon laser; M, mirror; CH, chopper; A, aperture; DM, dichroic mirror; F, filter; Defl, Beam deflection.

$$I = I_0 10^{-\varepsilon c l} \tag{1}$$

where I_0 is the incident beam power, I the transmitted power, ε the molar extinction coefficient, c the concentration of the analyte and l the optical pathlength. For a weakly absorbing analyte, $10^{-\varepsilon c l}$ can be approximated by $(1–\ln 10 \varepsilon c l)$ so that ΔI_A, the relative change in intensity, can be written as:

$$I_A = \frac{I_0 - I}{I_0} = \frac{I_0 - I_0(1 - \ln 10 \cdot \varepsilon c l)}{I_0} = \ln 10 \cdot \varepsilon c l \tag{2}$$

In single-beam TLS, there are two causes of intensity changes. One is the intensity reduction due to absorption of light by the analyte—the same as in absorption detection. The other is the decrease due to beam defocusing which causes less (light) power to strike the photodetector (see Fig. 6). This explains why in TLS the measured value of ΔI_A is higher than the value calculated on the basis of Eq. (2). To quantify this enhanced loss of signal intensity, an expression for the focal length of the thermal lens has to be found.

As noted above, if a laser beam is propagated through an absorbing sample solution, heat is released. Due to thermal diffusion, the heat will be drained from the laser beam centre to the surrounding solvent molecules. This will result in a cylindrically symmetric temperature distribution, with the axis of symmetry along the propagation direction of the laser beam. An RI profile with the same symmetry arises due to the dependence of RI on temperature, denoted as $\partial n/\partial T$. Since $\partial n/\partial T$ is negative for all solvents used in separation techniques, the RI of the solvent is lowest at the beam centre and increases to its value at ambient temperature at the boundary of the beam. This cylindrical RI profile acts as a negative lens that causes a defocusing of the propagating beam. The focal point of this (transient) lens, f_{TL}, is given by [39]:

$$f_{TL} = \frac{\pi \kappa \omega^2}{\ln 10 \cdot I_0(\partial n/\partial T) \cdot \varepsilon c l} \tag{3}$$

where κ is the thermal conductivity of the solvent and ω the radius of the laser beam. Eq. (3) shows that the thermal lens effect depends not only on the absorbance of the sample, but also on the laser beam characteristics and on the solvent. A strong thermal lens can be induced by choosing a high irradiance, I_0/ω^2. The values of κ and $\partial n/\partial T$ are more favourable for organic solvents than for water. As a result, the addition of an organic modifier—as is common in reversed-phase LC—causes higher TLS signals [47]. Some typical data for κ and $\partial n/\partial T$ are listed in Table 1. These are approximate values since there are differences in the data published by different workers. Furthermore, the values are influenced by temperature and measuring wavelength. They typically change a few per cent for a temperature change of a few degrees or for a wavelength change of some tens of nanometres. Therefore, the data in Table 1 are intended as estimates of relative sensitivities in TLS (or other thermo-optical) detection [48–51].

One should also note that the optimal position of

Table 1
Thermo-optical properties of solvents commonly used in normal-phase and reversed-phase LC (at 20 °C) and $\lambda = 589$ nm taken from Refs. [48–51]

Solvent	n	$\partial n/\partial T$ (-10^{-4} K^{-1})	κ (W m^{-1} K^{-1})	E[a]
Water	1.33	0.81	0.58	0.24
Acetonitrile	1.34	4.5	0.188	4.1
Methanol	1.32	3.94	0.202	3.3
Dichloromethane	1.33	5.5	0.122	7.6
n-Alkanes (C_5–C_{10})	1.36–1.41	4.2–5.5	0.118–0.141	5–8

[a] E, theoretical enhancement factor in TLS per mW of optical power, calculated using Eq. (7).

the (centre of the) sample cell is not at the focal point of the focusing lens (where the laser beam waist is at its minimum), but at the position where the waist has reached twice the minimum radius [39].

The intensity decrease due to the defocusing effect of the induced thermal lens in the sample cell at the optimal position is given by [41]:

$$I_{TL} = -\frac{\ln 10 \cdot I_0(\partial n/\partial T) \cdot \varepsilon c l}{\lambda \kappa} \quad (4)$$

and the total TLS signal by:

$$I_{TOT} = I_{TL} + I_A \quad (5)$$

Usually, in the literature dealing with TLS, Eq (5) is written as [41,44]:

$$I_{TOT} = I_A(1 + E) \quad (6)$$

where E is the enhancement factor of the response compared to Lambert–Beer's law. That is, E can be written as:

$$E = -\frac{\partial n/\partial T \cdot I_0}{\lambda \kappa} \quad (7)$$

E can be used to compare the performances of TLS and conventional absorption detection. Since E is proportional to I_0, it is advantageous to use high laser power. On the other hand, as noted earlier, I_0 should be limited, since non-linearity caused by saturation effects and/or photodestruction of analyte molecules must be avoided. Organic solvents such as acetonitrile and methanol are more suitable than water, because they show an about 5-fold higher $\partial n/\partial T$ and a 3-fold lower κ (see Table 1).

3.2. Instrumentation

The development of pump-probe (PP) techniques has led to major improvements in TLS. In this mode of TLS, a second (low-power) probe laser monitors the evolution of the thermal lens over time (see Fig. 6c) [52,55]. Pump-probe TLS (PP-TLS) has some interesting advantages. Firstly, it allows the use of a pulsed laser for the pump beam. This is impossible in single-beam (SB) TLS, since the build-up time of the thermal lens (10–100 ms) is much longer than the pulse duration (ca. 10 ns). Generally, an inexpensive low-power CW laser is used to detect the induced lens. Since most absorption bands of the analytes lie in the UV part of the electromagnetic spectrum and pulsed lasers easily provide output in that wavelength region, pulsed lasers are ideal for the pumping task. There are hardly any restrictions to the wavelength of the probe laser; it should fall within the sensitivity window of the detector and not be absorbed by the solvent. Secondly, lock-in detection—a popular signal-enhancing technique in optical pump-probe set-ups—can be applied. By amplitude modulation of the pump laser (for instance, by a mechanical chopper), the strength of the thermal lens—and, therefore, the resulting signal—will be modulated as well. By detecting only the modulated signal, S/N is improved [41]. Finally, HeNe or diode lasers can be used for probing so that the extra costs are marginal. Furthermore, such lasers are very stable, especially the diode lasers, so that their contribution to noise can be ignored.

A second development is double-beam (DB) TLS where a second, reference, beam is obtained by splitting the laser beam before transmitting the detector cell (cf. Fig. 6b). The intensities of both

beams are measured by two photodiodes. Their outputs are fed to a differential amplifier, for example the scheme proposed by Hobbs [56], so that the flicker noise of the laser is largely excluded and better LODs can be obtained.

TLS has also been applied using microscopy, denoted as thermal lens microscopy in the literature [57–59]. In this mode, small amounts of analytes (at the attomole level) can be measured in a single biological cell in vitro [58], but it can also be used for detection in chip-based systems [59].

3.3. Coupling to separation systems

It can be calculated from Eq. (7) that an enhancement factor of 10 can easily be achieved even if pure water is the solvent and a low power (30 mW) argon-ion laser (514 nm) is used for excitation. Therefore, TLS promises a high sensitivity when applied as a detection technique in μLC or CE, especially if organic modifiers are used. It will be possible to enhance E even further by using a laser that can deliver several Watts of optical power. However, there are several problems here. It should be realized that TLS in a dynamic system may be significantly different from TLS in a static system. Firstly, the build-up time of the thermal lens has to be considered, an aspect that is not included in Eq. (7) which has been derived for a static solution. Strong deviations from Eq. (7) can be expected when the peak width of the eluting or migrating sample is shorter than the thermal lens build-up time, t_c. Since, in general, t_c is on the order of 10–100 ms, and even in CE peak widths are typically as long as 1 s, the build-up time of the lens plays only a minor role. Unfortunately, the quality of the thermal lens is adversely affected by the flow: the heat production loses its radial symmetry and the resulting thermal lens becomes highly astigmatic. Furthermore, turbulence will cause considerable noise [44]. This means that E is much lower for dynamic compared to static systems. In practice, for static TLS measurements values of E are typically 20–50, while for flowing samples they are two to three times lower [60–63].

3.4. Practical usefulness

Table 2 shows that various research groups have explored the use of TLS as a detection technique for liquid separation methods. Conventional-size as well as micro, capillary and open-tubular LC, including ion chromatography (IC), have been studied and also CE, including micellar electrokinetic chromatography (MEKC). For convenience, also static, i.e., batch, experiments are included in the table. It should be emphasized, however, that the real use of TLS in analytical practice is still very limited. The examples shown in Table 2 are mainly about standard solutions. Nonetheless, there are some studies which deal with real-life samples, a fact that does not apply for all the other laser-based detection techniques considered in this review. In general, the objective of the cited papers is to show the enhancement factors that can be reached, the E values of Table 2 being the results quoted in those papers.

Some general conclusions can be drawn from Table 2. First of all, the E values for the SB mode are typically 3–10. For the DB mode, only one result is available, with an E value of 100. PP-TLS shows better performance than the SB mode as well: the enhancement here is typically 10–100. It should be remembered, however, that PP-TLS has the obvious disadvantage of being more complicated: a second laser (in all reported studies a HeNe laser) is required. Secondly, only one paper uses gradient LC [70]. This is not unexpected since a gradient will affect both κ and $\partial n/\partial T$ during the LC run, which will make it difficult to achieve adequate robustness. Thirdly, it should be realized that the E values refer to the wavelength provided by the (pump) laser, a fixed wavelength that in general does not correspond with the maximum of the absorption band. Consequently, the E values calculated above are only relevant for analytical practice (where absorption detection is invariably performed at the band maximum) if lasers become available that can be tuned to the band maximum. At present, this is still a serious barrier to implementing TLS in analytical practice.

The analytical performance of PP-TLS was studied by Šikovec et al. [75]. They compared the results obtained by PP-TLS and ICP-AAS detection coupled to IC and demonstrated that these were in good agreement. The authors reported an error margin of about 1% and an LOD of 0.1 $\mu g\ l^{-1}$ for PP-TLS detection in the analysis of (complexed) Cr(VI) in SRM samples. For AAS, these figures

Table 2
Survey of literature data on thermal lens detection coupled to separation systems

Analyte	TLS mode	Laser type	Wavelength (nm)	(Average) power (mW)	LOD		*E*	Refs.
					(n*M*)	($\mu g\ l^{-1}$)		
Static measurements:								
Clenbuterol (der)	PP	Ar^+	514	100	–	1.5	14	[60]
Cr(VI)	PP	Ar^+	514	160	–	0.1	10	[63]
V(V)	PP	Ar^+	488	120	0.3	–	100	[64]
Hydroxy-quinoline	PP	Ar^+	488	120	10 000	–	30	[64]
Pyrocatechol	PP	Ar^+	488	120	20 000	–	10	[64]
Nucleotides	PP	EDFA	1515–1590	~0.01	$>2\times10^6$	–	2–3	[65]
Conventional LC:								
Nitro-anilines	SB	Ar^+	488	190	–	20	1	[66]
Cobalt complex	PP	Ar^+	514	6	3000	–	~1	[67]
Nitro-anilines	PP	Ar^+	488	100	–	30	20	[55]
β-Carotene	PP	Ar^+	488	40	3	–	3	[68]
3-Chlorophenol	PP	F-centre	2400–3500	45	300	–	10	[69]
4-Chlorophenol	PP	F-centre	2400–3500	45	500	–	9	[69]
Clenbuterol (der)	PP	Ar^+	514	200	–	7	10	[61]
DNOC pesticides	PP	Ar^+	364	150	3	–	10	[70]
DNOC pesticides[a]	PP	Ar^+	364	150	20	–	3	[70]
Carotene (trans-β)	PP	Ar^+	476	60	–	0.1	100	[71]
Carotene	PP	Ar^+	476	60	–	0.6	100	[72]
Carotene	PP	Ar^+	476	60	–	0.5	100	[73]
Ion chromatography:								
Cu(II), Co(II)	PP	Ar^+	514	95	70–80	–	3–4	[74]
Cr(III)	PP	Ar^+	514	160	–	30	3	[74]
Cr(VI)	PP	Ar^+	514	160	–	0.3	3	[62]
Cr(III)	PP	Ar^+	514	160	–	10	10	[75]
Cr(VI)	PP	Ar^+	514	160	–	0.1	10	[75]
Fe(II)	PP	Ar^+	514	150	–	5	9	[76]
Fe(III)	PP	Ar^+	514	150	–	25	3	[76]
Micro-bore LC:								
Benzopurpurin	SB	Ar^+	514	90	–	3	24	[77]
Azobenzenes	DB	Ar^+	488	34	3	–	100	[78]
Amino acids (der.)	PP	Ar^+	488	300	80	–	100	[53]
Amino acids (der.)	PP	Ar^+	488	300	80	–	100	[54]
Electrophoresis:								
Amino acids (der.)	PP	HeCd	442	4	300	–	–	[79]
Amino acids (der.)	PP	Ar^+	458	130	50	–	1000	[80]
Amino acids (der.)	PP	KrF	248	5	500	–	>100	[81]
Lysine (indirect)	PP	HeNe	633	20	5000	–	–	[82]
AMP (nucleotides)	PP	Ar^+	257	10	50	–	30	[83]
Benzoic acid	PP	KrF	248	12	–	300	10	[84]
Preservatives	PP	KrF	248	12	–	~400	10	[84]
Amino acids (der)	PP	Ar^+	458	150	20	–	–	[85]
Open tubular LC:								
Nitro-anilines	SB	Ar^+	458	500	–	6000	10	[86]
Capillary LC:								
Ketones (der.)	PP	HeCd	442	3	>2000	–	–	[57]
Micellar electrokinetic chromatography:								
Nucleotides	PP	Ar^+	257	10	~50	–	30	[83]

[a] Gradient LC.

were 3% and 0.8 μg l^{-1}, respectively. Furthermore, linearity over the 0.5–100 μg l^{-1} range was reported for PP-TLS. That is, the analytical performance data were fully satisfactory. Performance data were also reported by Biosca et al., viz. on the determination of clenbuterol in pharmaceuticals [60] and in urine [61]. With PP-TLS detection the repeatability (expressed as RSD) was 1.5% for pharmaceuticals and 5.6% for urine (LOD, 7 μg l^{-1}). For the latter analysis, UV detection yielded a repeatability of 3.1%, but the LOD was 7-fold higher, i.e., 50 μg l^{-1}.

Another example of real-life analysis was reported by Franko et al. [71] and Luterotti et al. [72,73], who demonstrated the suitability of PP-TLS detection in the determination of β-carotene in fish body oil and vegetable oil, blood plasma and animal liver tissue. The authors report repeatabilities of about 4% (determined by the stability of the used laser), a linearity from 1 to 120 μg l^{-1} and an LOD of 0.1–0.6 μg l^{-1}, depending on the matrix. With UV detection, the LODs were about 100 times higher [71,72]. All these examples show that the repeatability is similar or somewhat worse for PP-TLS compared with UV detection, but the sensitivity is significantly better. An example of a chromatogram recorded by using TLS is shown in Fig. 7a, which reveals three peaks that were hidden in the chromatogram obtained with UV detection (Fig. 7b).

Remarkably, in some papers TLS is used in the (near-)IR region. As an example, in one study, tunable near-IR (NIR) radiation (1515–1590 nm) was obtained from a laser-diode-pumped (980 nm) Er-doped fibre [65]. An acousto-optical dispersive instrument was used to select the suitable wavelength. The NIR radiation was focused into the cuvette and the induced thermal lens was monitored by a HeNe laser. That is, absorption in the NIR region was converted into a response in the visible region, where detection can be performed more conveniently. Unfortunately, the LODs that were found for four nucleotides (dissolved in a mixture of deuterium chloride and deuterium oxide to avoid absorption by the OH bands of water) were rather disappointing, i.e., on the order of 1 m*M*. The poor sensitivity is due to the low absorbances of the nucleotides at NIR wavelengths and the low optical power (a few μW) of the NIR excitation beam. In another example an F-centre laser was used. Such a laser uses a crystal with crystal defects, denoted as colour (Ger: *Farbe*) or F-centres, as the laser material and provides tunable NIR radiation with several tens of mW of optical power. The improvement in terms of LODs is about one decade.

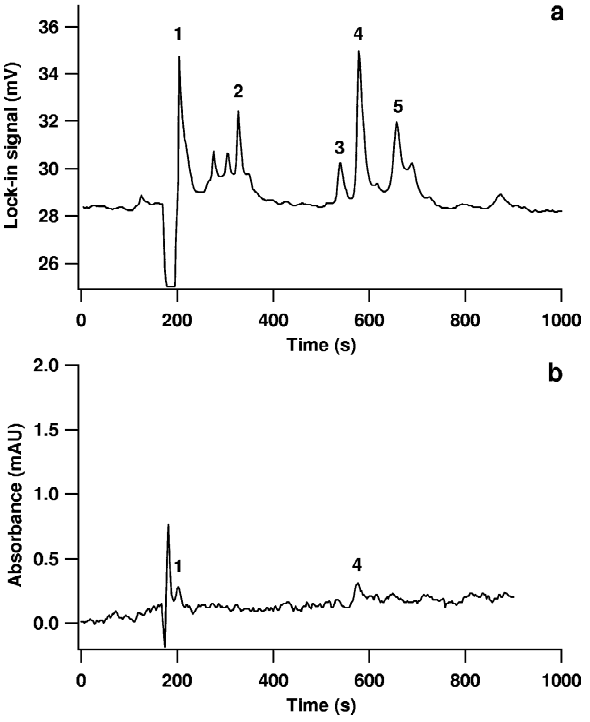

Fig. 7. Chromatograms of a 50-fold diluted extract of a pooled blood plasma sample obtained by LC with (a) TLS and (b) UV detection [71]. Peak identification: (1) lutein + zeaxanthine; (2) β-cryptoxanthine; (3) α-carotene; (4) *trans*-β-carotene; and (5) lycopen.

PP-TLS has also been coupled to CE. In contrast to LC, generally no organic modifiers are added to the (aqueous) buffers, so that the buffer solutions have less favourable κ and $\partial n/\partial T$ values and no spectacular enhancements is expected. Still, *E* values of 10–1000 are reported. The value of 1000 was achieved by using 50% of acetonitrile in the run buffer, which is quite exceptional [82]. As far as we know, no real-life samples were analysed using CE–TLS and no data are available on the repeatability and linearity of this combination.

4. Photoacoustic detection

Analogous to TLS, photo-acoustic detection (PA) is based on a temperature change induced by the absorption of radiation. In PA this change is monitored by measuring the accompanying effect on the pressure, which is detected by a piezo-electric transducer or a sensitive microphone and further amplified and processed [87–89].

4.1. Theoretical aspects

In PA, both CW and pulsed lasers can be used. The CW laser is usually modulated by means of a mechanical chopper so that a 50% duty cycle of the excitation beam is obtained. The theory of PA detection using a CW laser was developed by Kohanzadeh et al. [90]. If it is assumed that a focused laser beam propagates in a straight line, the time-averaged acoustic power, *P*, of the radially emerging pressure waves is given by [87,90]:

$$P = \frac{\beta^2}{c_p^2 \rho} \cdot \frac{P_L^2 \omega \varepsilon c l}{16} \tag{8}$$

where β is the volume temperature expansion coefficient, c_p the specific heat at constant pressure and ρ the density; these are all solvent parameters. P_L is the impinging laser power, and ω the chopper modulation frequency; these parameters should be considered as instrument characteristics. In fact, ε, the molar extinction coefficient, is the only characteristic of the analyte; c is the analyte concentration.

As regards the solvent parameters, these are similar for the organic solvents that are normally used in LC separations. Water is an exception; its c_p and ρ values do not differ very much from those of organic solvents, but its β value is approximately 5-fold lower [51]. Consequently, with water the achievable LODs will be some 10-fold higher than with organic solvents, which advocates against the use of the PA detection technique in CE.

The only laser parameter is the optical power, P_L, that, maybe unexpectedly, appears quadratically in Eq. (8). It is quadratic because not only the amplitude of the induced pressure wave is proportional to P_L, but the initial (radial) velocity of the pressure wave also depends on P_L. These two parameters, amplitude and initial radial velocity, determine *P*. Therefore, a laser operating at high power will be advantageous, although too high power may lead to self-defocusing and cause non-linear behaviour.

The modulation frequency of the chopper, ω, is important because it influences the signal intensity and also the signal processing part, since the modulation is part of the lock-in detection scheme. The performance of lock-in amplifiers is usually optimal at frequencies of 1 kHz and higher, close to the practical limit of operating a mechanical chopper (usually a few kHz).

Eq. (8) shows that the PA signal depends linearly on the analyte concentration. Furthermore, in contrast to TLS, PA is a zero-background technique. In the absence of analyte no pressure effect is induced by irradiating the sample. A pressure change will only occur if the sample has non-zero absorbance. As a result, the sensitivity of the technique depends almost exclusively on the collection efficiency of the PA signal.

For the pulsed-laser PA mode, the role of the above-mentioned parameters is similar. The only difference is the signal that has to be monitored: the peak amplitude of the pressure wave—i.e., the pressure change Δp—instead of the time-averaged acoustic power considered in the CW mode [87]. If it is assumed that the pulse profile is Gaussian and the induced pressure changes are small compared to the ambient pressure, Δp is given by [87,91]:

$$\Delta p = \frac{\beta}{c_p} \cdot \frac{4 E_L \varepsilon c l}{\pi \tau^2} \cdot \left(\frac{v_s E_L}{2 \pi r} \right)^{1/2} \tag{9}$$

where E_L is the pulse energy, τ the pulse width, v_s the sound velocity in the solvent and r the distance between the laser beam and the point at which the signal is observed.

The solvent parameters c_p and v_s, are essentially the same for all solvents commonly encountered in LC and CE separations. Also in this instance, due to the 5-fold lower value of β (cf. above), water is a less suitable solvent, but fortunately the influence of β is not as strong as in the CW mode.

It can be seen from Eq. (9) that a pulsed laser with a high peak power (large E_L combined with a short

τ) is favourable. If the pulse duration is short (<1 μs), side-effects such as self-defocusing (thermal lensing) do not play a role: these effects occur on a much larger time scale (typically in the ms range; cf. Section 3.3). Furthermore, Eq. (9) shows that, as in the CW mode, the PA signal is linearly related to the analyte concentration, c. Also in this mode, the transducer should be positioned as close as is possible to the point where the laser beam interacts with the solvent [88].

4.2. Instrumentation

It is not easy to predict whether a CW or a pulsed laser will give better LODs in PA. Under pulsed excitation conditions the generated pressure pulse is more compact; its dimension is roughly given by $v_s . \tau$, which is less than 1 mm for most combinations of lasers and solvents [88]. Under CW excitation conditions, the situation is markedly different. If a chopped CW laser is used, the on-time is on the order of 1 ms, which implies that the pressure wave will reflect several times against the walls of the detector cell during excitation. As a consequence, in the worst-case scenario, the sample cell can be brought in acoustic resonance and the quality of the detected signal will deteriorate. This suggests that, in PA, pulsed lasers are more favourable. On the other hand, the lack of a high duty cycle limits the sensitivity because the effective signal acquisition time is short. It should be noted that the final noise level depends on the detection mode utilized. With a CW laser random noise can be effectively suppressed by a lock-in detection scheme. If systematic noise dominates, a pulsed laser in combination with time gating is recommended: the noise can easily be separated from the signal by means of time discrimination [88].

The quality of the transducers largely determines the sensitivity in PA. Generally, piezo-electric transducers based on lead zirconate–titanate are used. The transducer is housed inside a metal cylinder so that it can be brought in close contact with the solvent in the detector cell. A typical flow cell for performing PA detection is shown in Fig. 8. In order to avoid contamination of the sample solution, the housing should be made of an inert material. Furthermore, its front surface should be highly reflective so that scattered laser light, upon being absorbed by the transducer, will not cause a false pressure change [88].

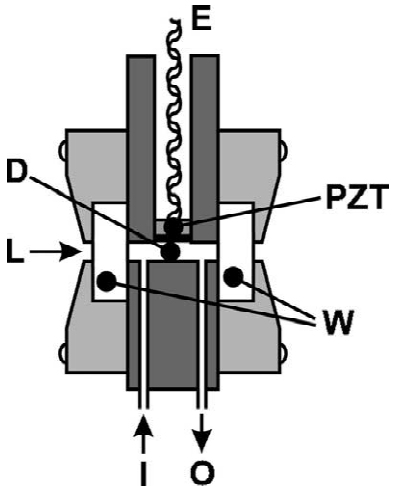

Fig. 8. Cell for photoacoustic detection [107]. Abbreviations: D, detection area; L, laser beam path; PZT, piezo element; W, quartz windows; E, electrical connection; I, effluent in; O, effluent out.

The transducer should be positioned as close as is possible to the focus of the exciting laser beam in order to create a strong signal. Since in LC and CE the chemical reactivity of the solvents is usually low, according to the literature the transducer can be installed inside the detector cell without serious risk of chemical interactions.

The transducer acts as a normal microphone so that its signal will be contaminated by noise from the surroundings. This noise can be eliminated by a lock-in amplifier (LIA) in the CW mode or by using time gating of the signal in the pulsed mode. In the CW mode—provided that acoustic resonance effects are avoided—the PA signal has the same modulation frequency as the mechanical chopper so that it can be detected by means of the LIA. Other frequency components, such as mechanical vibrations and sound from the surroundings, are regarded as noise and can be readily eliminated by the LIA. A more advanced approach of PA detection uses two identical transducers, a technique denoted as differential PA detection. The first one is positioned in close contact with the sample cell and the second one as close as is possible to the first transducer, but without acoustic contact so that it will not detect the

PA signal. Subtraction of the two outputs will create a ''clean'' signal, corrected for the noise from the surroundings [92].

In the pulsed-laser PA mode, a boxcar is usually used for time gating. Unwanted signals monitored by the transducer will arrive earlier or later than the desired signal and are therefore blocked. This holds for instance for signals caused by window absorption or echoes, which arrive later. Signals that are the result of scatter light absorption by the transducer compartment itself will, of course, arrive earlier [88].

Finally, the PA signals induced by pulsed lasers have a high acoustic frequency—a laser pulse as short as 1 μs may induce sound waves with a frequency of 1 MHz—far above the frequencies normally encountered in the surroundings, which are less than 10 kHz. Thus, by using a high-pass filter, such noise signals are effectively eliminated [88].

A rather exotic, but sensitive technique that was introduced a decade ago is capillary vibration induced by laser (CVL) [93,94]. When a capillary (i.e., the separation column) is irradiated by an intensity-modulated CW or pulsed laser beam [95], analyte molecules absorb radiation and periodically generate heat; hence, pressure waves are formed. These pressure waves cause the capillary to vibrate like a string. A schematic drawing of CVL is shown in Fig. 9. The capillary vibration can be monitored by measuring the deflection of a second (probe) laser beam (Fig. 9a) [93,94] or by a piezoelectric transducer (Fig. 9b) [95]. The authors claim very high *E* values of 100–1000, but the LODs unfortunately are in the micromolar range.

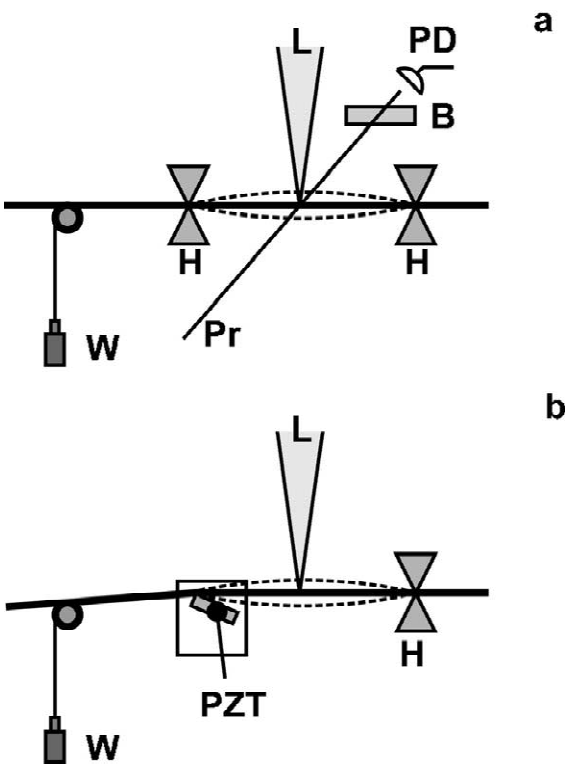

Fig. 9. CVL using (a) a second (probe) laser, (b) a piezo element for detection [93–95]. Abbreviations: L, pump laser beam; PD, photodiode; B, blade; H, holders; Pr, probe laser beam; W, weight; PZT, piezo element.

4.3. Coupling to micro-separation systems

Obviously, a PA detection cell—as schematically depicted in Fig. 8 above—can be readily used in static or flow experiments; its combination with conventional-size LC is also straightforward since geometrical constraints are not too serious. However, in micro-separation systems, the detection cell requires particular attention. It should be constructed from highly pure fused-silica in order to minimize false PA signals as a result of window absorption [88]. Moreover, its shape is critical: round detector cells are favoured from a separation point of view, since they can easily be constructed from capillaries normally used in CE and μLC. No connections to a detection cell, which introduce dead volume, are then needed [96]. Unfortunately, as far as PA detection is concerned, the curved walls of fused-silica capillaries strongly scatter the incoming laser beam, which causes unwanted illumination of the transducer. Furthermore, since in capillary cells external mounting of the transducer cannot be avoided, the overall performance of the detection system will be adversely affected. Several attempts have been made to design a flow cell which incorporates the transducer as close to the optical region as is possible, but the volume of such cells is a few μl, which is too large for micro-separation systems [97]. This explains the development of rather exotic detection modes such as CVL.

Since the signal-generation mechanism in CVL is somewhat different, this technique does not have the

disadvantage of false responses caused by scattered light. Furthermore, depending on the size of the capillaries, the laser-probed volume is 2–50 pl, and is therefore compatible with μLC and CE separations.

4.4. Practical usefulness

The number of publications dealing with PA detection (PAD) in liquid separation systems is very low and only a few groups were, or are, active in this field. Most of the data in Table 3 refer to static and FIA experiments and only a few papers deal with conventional-size LC [97,107]; the separation mode mainly studied is CE. To the best of our knowledge, real samples were not considered so far; all reported results in Table 3 refer to standard solutions.

In static experiments the enhancement factors in differential PAD are typically 3–10 and are not really impressive. In the context of this review, the results obtained with CE are more relevant. Interestingly, a 100-fold (and higher) enhancement has been reported for CE provided that CVL is applied as detection method. For CVL–PZT (signal detected with piezo

Table 3
Survey of literature data on photoacoustic detection

Analyte	PAD mode	Laser type	Wavelength (nm)	(Average) power (mW)	LOD		*E*	Refs.
					(n*M*)	(μg l^{-1})		
Static measurements:								
β-Carotene	Conv.	Ar^+	488/514	700	–	0.08	–	[98]
Cd(II)	Conv.	Ar^+	514	500	–	0.01	–	[99]
Vitamin A	Conv.	N_2	337	–	–	0.002	–	[100]
Chlorophylls	Conv.	N_2	337	26	–	~1	–	[101]
Dyes	Conv.	N_2	337	26	–	>1	–	[101]
Vitamin B	Conv.	N_2	337	26	–	4	–	[101]
Riboflavine	Conv.	N_2	337	26	–	10	–	[101]
PAHs	Conv.	N_2	337	26	–	0.2–7	–	[97]
Oil in water	Conv.	YAG	532	1 mJ*	–	10 000	–	[102]
Oil in water	Conv.	diode	904	2.3 μJ*	–	400 000	–	[102]
CrO_4^{2-}	Conv.	Xe-lamp	532	6	–	0.35	–	[103]
U(IV)	Diff.	dye	660	0.8–3.0 mJ*	800	–	<10	[92]
U(VI)	Diff.	dye	414	0.8–3.0 mJ*	1000	–	<10	[92]
Pu(IV)	Diff.	dye	476	0.8–3.0 mJ*	70	–	<10	[104]
Pu(VI)	Diff.	dye	831	0.8–3.0 mJ*	30	–	<10	[104]
Am(III)	Diff.	dye	503	0.8–3.0 mJ*	20	–	<10	[104]
Sunset yellow	CVL	Ar^+	488	70	100	–	>100	[93]
Sunset yellow	CVL-PZT	Ar^+	488	100	7	–	>1000	[105]
Flow injection analysis:								
NH_4^+ (der)	Conv.	Dye	610	1	–	8	3	[106]
PO_4^{3-} (der)	Conv.	Dye	880	1	–	70	~1	[106]
Fe(II) (der)	Conv.	YAG	532	1	–	30	~1	[106]
Conventional-size LC:								
Azobenzenes	Conv.	Ar^+	488	500	40	–	25	[107]
PAHs	Conv.	XeCl	308	40	>400	–	~1	[97]
Capillary electrophoresis:								
Riboflavine	CVL	Ar^+	476	40	2000	–	>1000	[94]
Phenylalanine	CVL	Ar^+	257	5–8	300	–	>1000	[94]
Tryptophan	CVL	Ar^+	257	5–8	30 000	–	>1000	[94]
Amino acids	CVL	Ar^+	488	–	10 000	–	~10	[108]
Phenylalanine	CVL-SW	KrF	248	10	100 000	–	>100	[95]
Tryptophan	CVL-SW	KrF	248	10	10 000	–	>100	[95]

* Average power unknown for pulsed laser, therefore pulse energy is listed.

crystal) [105] or CVL–SW (standing waves by capillary resonance) mode [95], an enhancement of two to three orders of magnitude is claimed. It should be noted, however, that only standard solutions were used to demonstrate the technique and, actually, only one group is working along this line. In addition, so far no data on the robustness of CVL detection or on precision and accuracy have been published.

Maybe it is illustrative for the state-of-the-art of PAD that the most recent paper included in Table 3 used a lamp-based system, i.e., a xenon lamp combined with conventional detection. The LOD reported under such, rather conventional, conditions is quite promising and comparable to results obtained by a laser–PAD system, i.e., 0.35 μg l^{-1} for chromate at 532 nm [103]. Admittedly, the study deals with static (cuvette) experiments and the bandwidth of the excitation light (100 nm) is far larger than in conventional UV detection (2–8 nm), which might result in non-linearity of the calibration plot since the requirement of Lambert–Beer's law of monochromatic radiation is violated.

5. Refractive index backscattering

Contrary to TLS and PA detection, RI detection—which is a universal detection method—is not based on light absorption by the analytes of interest. RI monitoring is done at a wavelength at which the analytes do not show any absorptivity [87]. Of special interest within the context of this review is refractive index backscattering (RIBS) detection, a special, laser-based, mode of RI, developed to be combined with micro-separation systems. Because of the very short pathlength in such systems, conventional RI detection cannot be used. It should be noted that RIBS is not the only laser-based RI detection method in micro-separation systems. Techniques based on interference and on light deflection were also studied in the literature and are discussed here as well.

5.1. Theoretical aspects

If it is assumed that the refractive index, n, of a mixture can be calculated by simply adding the refractive indices of the constituents multiplied by their mole fractions, one can write [87,109]:

$$n = \sum_i n_i x_i \tag{10}$$

where x_i is the mole fraction and n_i the RI of component i. Unfortunately, this equation is not valid. The relation between the mole fraction of an analyte and its RI response is non-linear because n is related to the polarizability [110]. Consequently, one should write:

$$\frac{n^2-1}{n^2+2} = \sum_i x_i \frac{n_i^2-1}{n_i^2+2} \tag{11}$$

Eq. (11) is valid only for mixtures of compounds that do not interact, as is usually true for non-polar molecules; otherwise cross-terms should be added. For a sample consisting of a single analyte in a solvent, and provided that higher order terms can be neglected, Eq. (11) becomes:

$$n = n_s + c\frac{(n_s^2+2)^2}{6n_s} \cdot \frac{M_s}{\rho_s}\left(\frac{n_a^2-1}{n_a^2+2} - \frac{n_s^2-1}{n_s^2+2}\right) \tag{12}$$

where n_s, M_s and ρ_s are the RI, molecular mass and density of the solvent, respectively, while c is the analyte concentration and n_a the RI of the analyte. Eq. (12) holds for an analyte concentration of less than about 10 mM, which poses no real limitation from an analytical point of view [87].

Eq. (12) shows that only analytes with an RI different from that of the solvent can be detected; the signal can be positive ($n_a > n_s$) as well as negative ($n_a < n_s$). LODs typically are 10^{-6} RIU (see Section 5.2) so it can be calculated from Eq. (12) that the corresponding LOD in concentration units is 0.3 mM for an analyte with $n_a = 1.40$ in pure acetonitrile ($n_s = 1.34$, cf. Table 1). Many analytes have an n_a of about this value, as can be seen in Fig. 10, so it can be safely stated that RI-based detection is not sensitive enough for trace-level concentrations. Even for an analyte with n_a as high as 1.55, the LOD is 0.1 mM.

RIBS is a laser-based technique developed for detection in capillaries [111]. It is based on interferometry: the difference in phase of two coherent light beams is monitored. Small optical pathlength differences result in constructive or destructive inter-

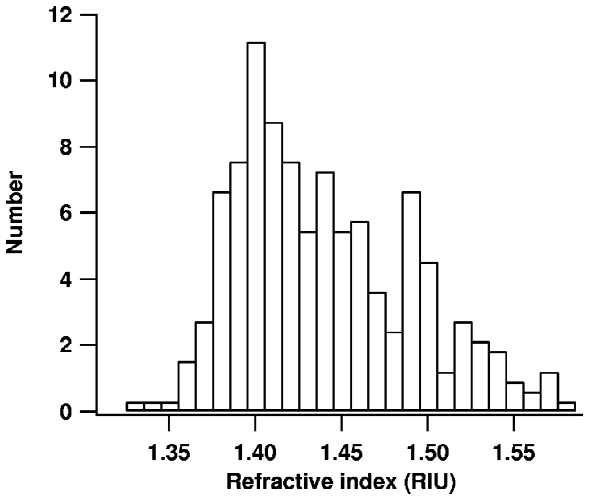

Fig. 10. Distribution of refractive indices of some 100 organic compounds that can be regarded as model analytes. Data from Ref. [51].

ference of the two beams and, hence, in a bright signal or in almost complete darkness. A schematic is shown in Fig. 11a. The pathlength differences are introduced by the two outer (air/glass) and inner (glass/liquid) boundaries of the capillary; axial illumination of the capillary results in a fan of light being scattered from these four boundaries perpendicular to the capillary axis. If we regard the capillary cross-section as a Fabry–Perot interferometer, it can be shown that for constructive interference, the following condition has to be fulfilled:

$$\cos\alpha = \frac{k}{2nd} - 1 \qquad (13)$$

where α is the refractive angle, k any integer number and d the core diameter. Eq. (13) shows that there are multiple solutions for α, each one corresponding to a fringe with maximum intensity. RIBS detection is based on the fact that the position of the fringes will shift if analyte molecules pass through the irradiated volume. As will be obvious from Eq. (13), a change of n due to the elution or migration of an analyte-containing zone will cause a change of α, and the interference fringes will be displaced. This shift can be quantified and is a measure for the change in refractive index (Δn), and, hence, for the presence of an analyte in the LC or CE effluent.

Treating the capillary as a Fabry–Perot interferometer is, however, only a crude approximation. The inner boundaries are strongly curved spherically and do not have the parabolic curvature of the mirrors usually encountered in Fabry–Perot interferometers. Furthermore, the reflections at the outer boundary of the capillary cannot be ignored. In practice, these reflections will be much stronger than those at the core boundaries, since the outer boundary deals with an air–glass transition which has a larger RI difference (about 0.45 RIU) than the glass–liquid boundary (usually less than 0.25 RIU). As a result, the interference pattern is much more complex than is suggested by Eq. (13). In practice, the main effort in RIBS detection development has been devoted to the reduction of the background caused by the reflections [111].

5.2. Instrumentation

An improvement of the set-up of RIBS detection over the original design by Bornhop and Dovichi [112] was proposed by Bruno et al., who immersed the detection part of the capillary in an RI matching glue [111]. The outer glass–air boundary is now replaced by a glue–glass boundary and since there is

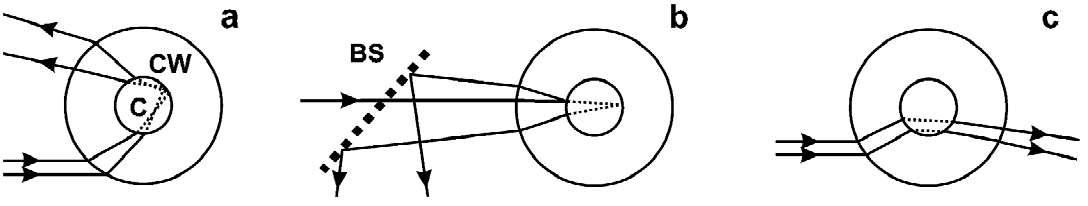

Fig. 11. Cross-sectional view of raytracing through a separation capillary. (a) RI backscattering; (b) retro-reflection; (c) beam deflection. Abbreviations: C, core; CW, capillary wall; BS, beam splitter. The dashed lines indicate the pathlength differences that are introduced when the RI of the liquid (which flows through the core) changes.

no difference in RI, reflections caused by the outer boundary are absent. The interference fringes now show up solely as the result of the reflections at the inner liquid–glass core boundary. This greatly simplifies the interference pattern and furthermore makes the position of the light-sensitive detector less critical. Another advantage of this approach is the insulating property of the index-matching glue: temperature changes of the surroundings have less influence on the signal.

Despite these improvements, temperature fluctuations that induce RI changes are still the largest source of noise in RIBS. As can be read from Table 1, for most solvents $\partial n/\partial T$ is on the order of 10^{-4} RIU/K. This implies that an LOD of 10^{-7} RIU can only be achieved if the thermal stability is better than 10^{-3} K. Especially in CE, where Joule heating takes place inside the capillary core as a consequence of the separation current, such a high degree of temperature stability is difficult to achieve.

Since RIBS places essentially no restrictions on the wavelength applied and low optical powers can be used, a HeNe laser is a good choice as the light source. Such lasers have a good operation performance (less than 1% flicker noise and a coherence length up to 30 m), are inexpensive and, last but not least, easy to operate. As has been shown in the literature, even diode lasers can be used for RIBS [114,115]. This seems surprising since, contrary to HeNe lasers, the wavelength of diode lasers is strongly dependent on the operating current and temperature. Fluctuations in these parameters can cause ''mode-hops'' from one to another longitudinal oscillation mode and, thus, changes in laser wavelength [116]. Evidently, this will cause changes of the fringe position and disturb the RIBS signal, so that a very stable power supply is needed to prevent them. Diode lasers have some distinct advantages over HeNe lasers that make them especially useful for RIBS measurements: they are extremely small-sized and their flicker noise is less than 0.01% or two decades better than that of HeNe lasers.

Detection is generally performed by using the brightest interference fringe. As outlined above, an RI change induces a displacement of the fringe, which is recorded by a position-sensitive device. Three devices are used: a conventional photodiode in combination with a pinhole, a position-sensitive photodiode (PSD), and a linear photodiode array (which has its light-sensitive elements in one dimension) or a charged-coupled device (CCD) camera, which has its elements in two dimensions.

The combination of a photodiode and a pinhole or slit is easy to construct and is inexpensive; the LODs obtained are $2–6\times10^{-7}$ RIU in FIA experiments [117,118]. In the second device, the light-sensitive area is divided into two (or more) regions: a left (L) and right (R) part. The photocurrent induced by the L part is subtracted from that induced by the R part, so that for a properly centred fringe, the photocurrents will cancel and a zero signal is obtained. If the centre of the fringe moves off-centre, the signal becomes non-zero, its sign being determined by the direction of the fringe shift. Due to the cancellation effect of the photocurrents, the flicker noise is considerably reduced. Because no light is lost as in a photodiode–pinhole combination, a better S/N can be obtained. A PSD usually performs better than a system with two separate photodiodes since PSDs are made from a single chip of silicon so that their characteristics are more constant over the light-sensitive area of the device [111]. In a FIA experiment (selected to eliminate the influence of the separation system), the LOD obtained using a PSD was as low as 7×10^{-8} RIU.

In the third device, a linear photodiode array is used to measure the position of more than a single fringe so that a positional change can be measured more accurately. A CCD can be applied as well, but since the positional change of the fringes is in one dimension, the second dimension provided by a CCD is not utilized. Of course, the CCD elements (pixels) in the second dimension can be added so that the noise contribution of each individual pixel to the signal will be reduced.

With capillary isoelectric focusing (CIEF) separations, all the zones with focused analytes can be acquired at the same time when using a CCD [119,120]. A CCD also allows real-time analysis of the fringe pattern; next to positional changes the modulation depth (the normalized difference in intensity of the nodes and anti-nodes) of the interference pattern is also taken into account [121–123]. By real-time fitting of the intensity profile RI changes can be measured more accurately which should improve the quality of the signal. For CE–

RIBS an LOD of 1.4×10^{-6} RIU was found when using real-time analysis [123].

It is interesting to consider whether alternatives for RIBS perform better. One study discusses a detection system that is based on interference from retroreflected beams (RR). RIBS and RR are very similar because interference is measured from reflected beams in both instances (viz. Fig. 11b) [124]. In RR, however, the reflected beam retraces the same path as the (focused) laser-beam, so that a beam splitter is needed to separate the beam to be measured. LODs in CE are on the order of 10^{-6} RIU, i.e comparable with the LODs obtained with RIBS. Detection based on laser-beam deflection (viz. Fig. 11c) does not provide better results: the LOD in μLC is 1×10^{-6} RIU [96,113]. Finally, in RIBS index matching fluids have been used for FIA and CE. Here, the LODs were found to be 7×10^{-8} and 4×10^{-6} RIU, respectively.

5.3. Practical usefulness

Table 4 lists all papers dealing with RIBS as well as other RI modes applied to micro-separation systems. For convenience, some FIA results were included. There are, of course, no data on enhancement factors compared with absorption detection: RI detection is not based on light absorption and, actually, is of special interest to detect analytes that cannot be detected by absorption at all. Instead, LODs expressed in μRIU are included.

In cIEF, the zone of focused proteins is usually detected by an on-column detector during a mobilization process: salts are added to one end of the capillary so that the gradual progress of the pH shift in the capillary causes the protein zones to migrate. This process causes the migration times to vary 10–15%. Since the RSD of each zone position is better than 1%, the repeatability of such cIEF experiments is much better by directly acquiring the protein zones using beam deflection measured by a CCD. Adding p*I* markers is not necessary once the relation between p*I* and the position of a zone is known [119].

Especially with RIBS detection, LODs in terms of Δn are in the 10^{-6} RIU range—even in CE where temperature effects play an important role—so that further improvements will not easily be achieved (cf. Section 5.2). This does not yet hold for the chip-based system of Swinney et al. [115] where the LOD is 10^{-5} RIU. Presumably, the thermal stability can be further enhanced here so that a 10-fold improvement of LODs should be expected.

All data quoted in Table 4 refer to standard solutions, except for the determination of caffeine in food [122]. The authors found caffeine concentrations of 100–250 mg l^{-1} in coffee and coke; the linearity of the calibration plot was somewhat better than for UV detection over the range measured (r, 0.98 and 0.99 for UV and RIBS, respectively). To our best knowledge, these are the only published analytical performance data for the techniques considered here.

6. Raman spectroscopy

Raman spectroscopy (RS) is a laser-based technique that became a versatile analytical tool in the last decade, mainly because of recent instrumental developments in the field of laser technology and detection system such as CCDs [22,23,127]. Raman signals are obtained by irradiating a sample with monochromatic radiation and measuring the small portion of scattered radiation that is inelastic, i.e., has shifted in wavelength. The shifts, which are both positive and negative, depend on the molecular structure and the vibrational transitions of the molecules that are involved in the scattering; that is, Raman spectroscopy is a mode of vibration spectroscopy. Its vibrational information has, in principle, an analyte identification potential similar to that of IR spectroscopy. However, in contrast to IR, RS can be used for aqueous solutions, which is highly beneficial for on-line detection in LC and CE.

6.1. Theoretical aspects

In RS the inelastic scatter of laser light caused by the analyte is measured. Light absorption as such does not play a role. Molecular vibrations will show up in the Raman spectrum if a change in the polarizability, α, of the analyte molecules is induced. In this respect, RS is more or less complementary to IR: in IR vibrations show up that cause a change in electric dipole moment while in RS the polarizability should change. The latter holds for all vibrations that modify the symmetry of the associated electron

Table 4
Survey of literature data on laser-based RI detection coupled to separation systems

Analyte	RI mode[a]	Laser type	Wave-length (nm)	LOD			Refs.
				(μM)	(mg l^{-1})	(μRIU)	
Flow-injection analysis:							
Glycerol	Defl.	HeNe	633	–	–	3	[112]
Glycerol	RIBS	HeNe	633	–	–	0.6	[117]
Glycerol	RIBS	HeNe	633	–	1	0.2	[118]
Glycerol	RIBS	diode	670	1000	–	–	[123]
Mandelic acid	RIBS	diode	670	1000	–	–	[123]
Glucose	RIBS	diode	670	800	–	–	[123]
Saccharose	RIMF	HeNe	633	10	–	0.07	[111]
Micro-bore LC:							
Alkylbenzenes	Defl.	HeNe	633	–	240	1	[96]
Glucose	Interf.	HeNe	633	–	20	3	[113]
Saccharose	Interf.	HeNe	633	–	20	3	[113]
Raffinose	Interf.	HeNe	633	–	20	3	[113]
Capillary electrophoresis:							
Saccharose	Defl.	HeNe	633	0.7	–	0.03	[125]
Organic dyes	RIBS	HeNe	633	0.5	–	–	[121]
Maltose	RIBS	HeNe	633	13	–	1.4	[122]
Lactose	RIBS	HeNe	633	30	–	1.4	[122]
Ribose	RIBS	HeNe	633	70	–	1.4	[121]
Caffeine	RIBS	HeNe	633	2	–	>0.1	[122]
Saccharose	RIMF	HeNe	633	–	–	4	[111]
Lactose	RIMF	HeNe	633	–	–	4	[111]
Cs(I), Li(I)	RIMF	diode	675	0.1–1	–	2	[114]
Ba(II), Mn(II), Co(II), Zn(II)	RIMF	diode	675	0.1–1	–	2	[114]
Mg(II)	RIMF	diode	675	0.01–0.1	–	2	[114]
Saccharose	RR	HeNe	633	–	–	2	[124]
Maltose	RR	HeNe	633	–	–	2	[124]
Lactose	RR	HeNe	633	–	–	2	[124]
Capillary iso-electric focusing:							
Phosphorylase	Defl.	HeNe	633	0.2	–	–	[126]
Ovalbumin	Defl.	HeNe	633	0.4	–	–	[126]
Hemoglobin	Defl.	HeNe	633	0.8	–	–	[119]
Carbonic anhydrase II	Defl.	Ar^+	514	–	5	–	[120]
Chip-based separation systems:							
Glycerol	RIBS	HeNe	633	4000	–	50	[115]
Glycerol	RIBS	diode	670	700	–	10	[115]

[a] RI detection using laser beam deflection (Defl.), interferometry (Interf.) or RI matching fluid (RIMF).

cloud. When α_0 is the polarizability at the equilibration distance, r_{eq}, then the influence of a specific vibration on α can be approximated by [128]:

$$\alpha = \alpha_0 + \frac{\partial \alpha}{\partial r}(r - r_{eq})\cos\,\omega t \quad (14)$$

where ω is the frequency of the vibration, $r - r_{eq}$ its amplitude and t the time. When an electromagnetic field (the laser beam) with amplitude E_0 and frequency ω_{ex} interacts with the molecule, an electrical dipole moment, m, is induced:

$$m = \alpha E = \left[\alpha_0 + \frac{\partial \alpha}{\partial r}(r - r_{eq})\cos\,\omega t\right] \cdot (E_0 \cos\,\omega_{ex} t) \quad (15)$$

By rewriting Eq. (15) as:

$$m = \alpha_0 E_0 \cos(\omega_{ex} t) + \frac{E_0(r - r_{eq})}{2} \frac{\partial \alpha}{\partial r} [\cos(\omega_{ex} - \omega)t + \cos(\omega_{ex} + \omega)t] \quad (16)$$

it becomes clear that m comprises three frequencies, ω_{ex}, $\omega_{ex} + \omega$, and $\omega_{ex} - \omega$. The first one represents Raleigh scatter and corresponds to radiation with the same frequency as the incident radiation. The other frequencies correspond to the Stokes ($\omega_{ex} - \omega$) and anti-Stokes ($\omega_{ex} + \omega$) shifts; conventional RS deals with the Stokes region. The anti-Stokes peaks, especially the larger vibrational frequencies, are less intense, a phenomenon that cannot be seen from the classical approach in Eqs. (14)–(16); in practice they are hardly considered in RS.

RS has some inherent disadvantages. The most obvious one is the low sensitivity—RS is based on inelastic light scattering, a very inefficient process. The signal intensities are proportional to λ^{-4}, that is, they are strongly enhanced at short wavelengths. Unfortunately, at short wavelengths the fluorescence background becomes a serious hindrance. Within this context an unexpected feature is worth to be emphasized: it has been shown in the literature that in the deep UV (excitation below 260 nm) fluorescence interference is no longer a problem [129].

In order to improve the sensitivity of RS, special modes of Raman spectroscopy can be exploited, such as resonance RS (RRS) and surface-enhanced RS (SERS) or even their combination, surface-enhanced resonance RS (SERRS). Both surface enhancement and resonance have a significant signal-enhancing potential. In RRS, the signal-enhancing mechanism is the coupling of the vibrations to an electronic transition; the sensitivity gain over conventional RS is about 10^3 [130]. It can be applied to analytes which have a significant molar absorptivity at the available laser wavelength. Two features are noteworthy here: (i) only a limited number of vibrations shows up in the spectrum because only the vibrations that are affected by the electronic transition are amplified and (ii) analyte fluorescence is a serious problem. In fact, the use of RRS for analytical purposes is still in an exploratory stage; deep UV–RRS probably has the brightest future since it will be widely applicable (cf. Fig. 1) and the fluorescence background is only marginal [129]. In SERS, the analytes have to be adsorbed on a metallic substrate, usually a silver colloid. In favourable cases the signal is intensified by 10^5–10^6 without a serious simultaneous increase of the background: the silver particles also cause fluorescence quenching [131,132]. Unfortunately, SERS is less widely applicable than conventional RS since not all analytes are adsorbed to the (negatively charged) silver colloid particles. However, for adsorbing compounds, spectacular results can be achieved in SERRS wherein resonance and surface enhancement effects are combined. For example, the detection of single molecules of Rhodamine 6G adsorbed on nanoparticles of a colloid silver solution has been claimed by Nie and Emory [133].

6.2. Instrumentation

In the three modes of RS, the choice of the laser is of utmost importance. Though there is little restriction on the laser wavelengths to be used for conventional RS, background fluorescence, which will obscure the RS signals, should be avoided as much as possible. Therefore, red or NIR (785 nm) lasers are preferred, usually combined with CCD detectors that are sensitive in this wavelength region. Another approach is Fourier-transform RS, a technique similar to FT-IR that received much attention in the last decade for analytical purposes [134]. It provides good-quality spectra, despite the long wavelength used—1064 nm provided by a Nd:YAG laser. Under these conditions fluorescence is essentially absent and, in addition, photodecomposition does not occur, so that high laser powers can be used.

As indicated above, in SE(R)RS and deep UV–RRS the fluorescence background is strongly reduced which makes these RS modes very attractive from an analytical point of view. When excitation is performed in the deep UV (below 260 nm), one can often benefit from the high Raman cross-sections at these wavelengths and the signal-enhancing capabilities of RRS, since a wide range of analytes have absorption bands in this wavelength region [129,135]. Recently, lasers suitable for providing radiation in this wavelength region became commercially available, i.e., intracavity frequency-doubled

argon-ion lasers that provide radiation of 229, 244 and 257 nm.

To reject the Rayleigh scattering, triple spectrographs are often used. However, these are known to be very inefficient as far as light throughput is concerned. Especially in the deep UV, transmissions of these spectrographs are about 1–3% or less [136]. As an alternative, dielectric stack filters can be used which attenuate the Rayleigh scattering approximately 1000-fold, so that a single spectrograph can be used for recording the Raman spectra [136].

6.3. Coupling to separation systems

It should be noted in advance that—contrary to the other laser-based detection methods discussed here—RS is intended to be a method of identification, which can be combined with both conventional-size LC and micro-separation systems. In principle, there are no special requirements to be fulfilled for the on-line coupling of liquid separation techniques and conventional RS. Water is the preferred solvent since—compared to other liquids—it is a poor Raman scatterer. From this point of view, CE and RS form a perfect combination. In LC the situation is less favourable: the Raman spectra of the modifiers may interfere with the analyte spectra so that spectral subtraction procedures have to be applied.

Despite what was said above, the on-line coupling of CE or LC and RS itself is not really straightforward. Usually the sensitivity provided by RS is not sufficient to detect analytes at the concentration levels typically studied with these techniques. This explains why in CE emphasis has been on analyte enrichment using isotachophoresis in order to meet the RS conditions [137–139].

In conventional-size LC–RS, the use of recently developed liquid-core waveguide (LCW) cells is studied to improve the sensitivity [136,140,141]. The detector cell should have an optical pathlength of, typically, 50 cm but an internal volume of no more than about 20 μl to avoid undue band broadening. The LCW allows highly efficient light-guiding through a small-bore (200 μm I.D.) capillary, since the RI of the cell material, PTFE AF2400, is 1.29, which is lower than that of solvents used in LC, such as water, acetonitrile and methanol, which have RIs of around 1.33 (cf. Table 1). The RS signal can be collected in the ''forward'' or ''backward'' configuration. In the forward mode, the laser light is coupled into the LCW on one end and the RS signal is collected at the other end. In the backward mode, the focusing of the laser beam into the LCW and the signal collection is done at the same side.

Presumably because of the serious fluorescence background problem, till now LC–RRS hardly received attention in the literature (see below). Emphasis has been on at-line approaches involving a spray jet interface directed on the use of SE(R)RS [142–144]. After the LC separation, the effluent is deposited on a solid substrate (for instance, a TLC plate), a silver colloid is added and SE(R)RS spectra are recorded.

6.4. Practical usefulness

In Table 5, relevant data on the coupling of RS and its special modes with liquid separation systems are shown. The first attempts to effect the on-line coupling of conventional RS and LC underlined the huge sensitivity problem; emphasis is fully on detection while recording of analyte spectra for identification purposes is still out of scope. For example, Nguyen Hong et al. explored the potential of conventional-size LC–RS by using as much as 1 W of optical power from an argon-ion laser [146]. Nevertheless, they had to report an LOD of 10 μg toluene in an injected sample of 20 μl. In a study on μLC, Cooper et al. used a HeNe laser and a CCD detector, applying deuterated solvents to increase the Raman window [154]. They found an LOD of 75 ng nitrobenzene in an injected sample of 60 nl. Obviously, these results are discouraging and suggest that on-the-fly scanning of RS spectra needs extremely high analyte concentrations.

The new approach in the direct coupling of LC with conventional RS via LCW waveguides was explored by Dijkstra et al. [140,141]. They used LCWs of 50 cm length that did not deteriorate the resolution in conventional-size LC. The LODs for some nitro compounds ranged from 10 to 500 mg l^{-1} [140]. The calibration curve was linear over two decades (r, 0.997). More importantly, the authors were able to record Raman spectra at the 0.5 g l^{-1} level. Very recently, they applied the same technique to a mixture of nucleotides, adenine, guanosine and

Table 5
Survey of data on Raman spectroscopy coupled to separation systems

Analyte	Raman mode	Laser type	Wavelength (nm)	(Average) power (mW)	LOD		Ref.
					(μM)	(mg l^{-1})	
Flow-injection analysis:							
Propanol	Conv.	diode	785	60	–	2	[145]
Conventional-size LC:							
Toluene	Conv.	Ar^+	514	1000	–	480	[146]
Xylenes	Conv.	Ar^+	488	3000	10	–	[147]
Nitro-aniline	Conv.	Ar^+	514	40	–	10	[140]
Alkanols	Conv.	diode	785	60	–	2	[145]
Nucleotides	Conv.	HeNe	633	32	–	100	[141]
Benzene	Conv.	diode	785	60	–	6	[148]
Azooxybenzenes	Conv.	Ar^+	458/514	700	1000	–	[149]
Nucleotides	SERS	Ar^+	514	10–12	16	–	[150]
Dyes	SERS	Ar^+	514	100	0.15	–	[151]
Drugs	SERS	Ar^+	488	85	–	100	[152]
PAHs	RRS	Ar^+	244	70	–	0.02–0.05	[136]
Cathionn dyes	SERRS	Ar^+	514	15	–	0.08	[143]
Anionic dyes	SERRS	Ar^+	514/458	–	–	5–10	[144]
Dyes	SERRS	Ar^+	514	17	–	0.05–0.25	[142]
Nitrophenols	SERRS	Ar^+	458	41	–	0.014	[153]
Micro-bore LC:							
Nitrobenzenes	Conv.	HeNe	633	25	–	1300	[154]
Dyes	RRS	Ar^+	488	400	–	1.5 ng	[155]
Capillary electrophoresis:							
Amino acids	Conv.	YAG	532	300	1000	–	[156]
NO_3^-, ClO_4^-	Conv.	YAG	532	300	10	–	[157]
Chlorophenols	SERS	HeNe	633	20	–	1000	[158]
Amino acids	SERS	HeNe	633	20	–	1000	[158]
Dyes (R6G)	SERS	Ar^+	514	–	>0.01	–	[159]
Riboflavin	SERS	Ar^+	514	17	1	–	[160]
Dyes	SERS	YAG	532	300	10	–	[156]
Dyes	RRS	HeCd	442	40	3	–	[161]
Isotachophoresis:							
Nucleotides	Conv.	YAG	532	400–700	5	–	[137]
Nucleotides	Conv.	YAG	532	2000	20	–	[138]
Herbicides	Conv.	YAG	532	500	>0.06	–	[162]
Herbicides (on chip)	Conv.	YAG	532	2000	–	0.06–0.08	[139]

uridine 5′-monophosphate [140]. When an aqueous eluent was used with no organic modifier, the limits of identification for these analytes were in the 0.1–0.5 g l^{-1} range.

LC has also been coupled on-line with RRS. μLC–RRS with excitation in the visible range was performed for some dyes. Interference of fluorescence is then a main problem. The LOD in absolute mass units was 1.5 ng [155]. Very recently, LC–deep UV–RRS was explored with a mixture of PAHs as model compounds [136]. The results are depicted in Fig. 12. They underline the potential of the coupling mode: LODs were 15 to 50 μg l^{-1}.

The on-line combination of LC and SE(R)RS suffers from compatibility problems of separation and colloid conditions. Nonetheless, it has been successfully applied [150,152]. For a standard mixture of nucleotides, LODs were as low as 16 μM [150]. Obviously, such compatibility problems are far less serious when LC and SE(R)RS are coupled

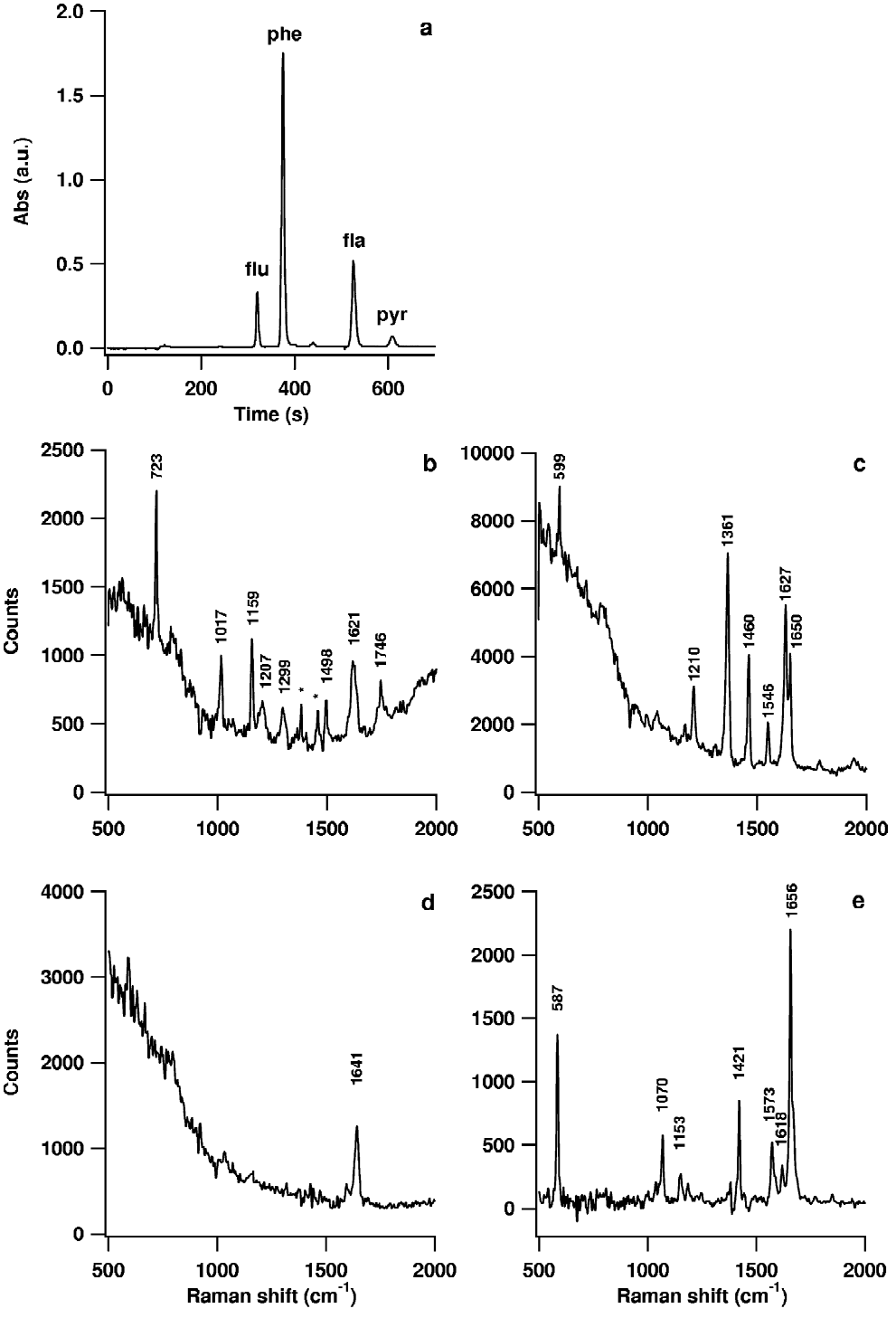

Fig. 12. LC–RRS of four PAHs [136]. (a) LC–UV chromatogram. Resonance Raman: (b) fluorene, (c) phenanthrene, (d) fluoranthene, and (e) pyrene. The spectra were corrected for the eluent background (peaks with asterisks originate from the background spectrum), self-absorption, and transmission profile of the dielectric stack filter.

at-line. Using a silica TLC plate as the substrate, at-line LC–SE(R)RS was successfully used for both cationic and anionic dyes, though the latter group is not easily adsorbed to the negatively charged silver colloid particles [142–144]. Using an ion-pair LC separation does not negatively influence the deposition process or the SE(R)RS results. In at-line LC–SER(R)S the identification potential of Raman spectroscopy can be fully exploited. For both types of dyes, characteristic spectra were obtained at a level of 50–250 $\mu g\ l^{-1}$ [142].

In CE, as was already noted above, isotachophoresis is an interesting option for analyte enrichment. This was demonstrated by Morris et al., who separated nucleosides [137,138] and herbicides [139,162]. Enrichment factors up to 3000 were achieved so that conventional RS could be applied; LODs were in the low micromolar range. He et al. studied at-line CE–SERS [158]. The authors evaluated the separation and detection with the CE–SERS system using two amino acids, tyrosine and tryptophan, and a chlorophenol mixture at a concentration level of about 1 $g\ l^{-1}$.

To the best of our knowledge, only standard solutions were analysed. No data on repeatability and dynamic range is available. In view of the identification potential of RS and its modes, differences between spectra of similar compounds can only be observed when the spectra are recorded at concentration levels that are 10–100-fold higher than the LOD, thus in the m*M* or $g\ l^{-1}$ range. Furthermore, libraries of RS at typical wavelengths are not yet available.

7. Degenerate four-wave mixing

Four-wave mixing (4WM) is based on the interaction of three laser beams in a gas, liquid or solid medium [163]; upon absorption of light a fourth beam is created, the signal beam which emerges in a well-defined direction. In the field of 4WM, popular techniques in physics are optical phase conjugation [164] and coherent anti-Stokes Raman spectroscopy (CARS) [165]. In degenerate four-wave mixing (D4WM)—the technique considered in this paper—the interacting beams have the same wavelength. D4WM was originally used as a spectroscopic means to study atomic vapours [166], and became popular in combustion research [167]. In the past two decades, D4WM was also used to study liquid crystals [168], semiconductors [169], thin dye films [170] and plasmas [171]. In the last decade, the potential of D4WM as a sensitive detection method in combination with liquid separation systems has been explored. The analytical interest can be readily understood. In principle, D4WM is a zero-background technique: upon absorption of light, a signal is created on a dark background which can be efficiently detected because of its directionality [172].

7.1. Theoretical aspects

Like TLS, D4WM is a thermo-optical detection method [173]. It is based on the interference of laser light, which is obtained by splitting a laser beam in two pump beams, and subsequent recombination of the beams in a detection cell. Laser light absorption by analyte molecules only occurs at the planes of constructive interference. As a result of non-radiative relaxation of the excited analyte molecules, the heat delivered to the surrounding solvent molecules produces a spatial modulation of the refractive index, *n*, which is temperature dependent, as was outlined in Section 3.1. The periodic refractive index profile thus created is an equivalent of a holographic grating from which a third beam, denoted as the probe beam, can diffract. Diffraction of the probe beam produces the D4WM signal beam which is, in contrast to many other laser techniques (laser light scattering, LIF and Raman spectroscopy), as directional as a laser beam [172,174].

The interference pattern created by the two pump beams can be readily calculated. If the interaction angle is 2θ, then the distance between the planes of constructive interference (Λ) obeys the following expression:

$$\Lambda = \frac{\lambda}{2 \sin \theta} \tag{17}$$

Of course, for the refractive index grating the fringe distance is Λ as well.

Two optical configurations are used to generate a D4WM signal, i.e., a forward (F) and a backward

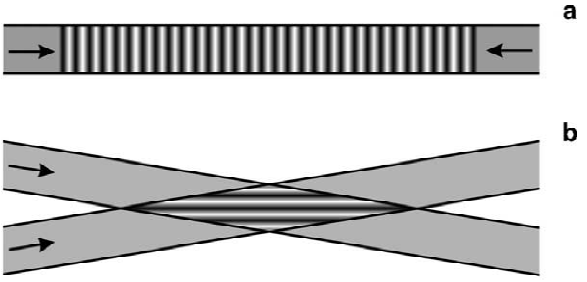

Fig. 13. Beam directions and overlap area in (a) B-D4WM and (b) F-D4WM.

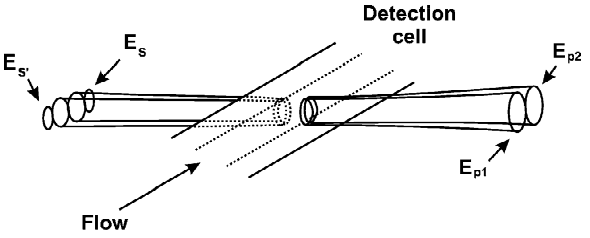

Fig. 14. Detailed picture of F-D4WM. E_{p1} and E_{p2}, (focused) pump beams; and E_s, signal beam. $E_{s'}$ is a signal beam as well, but ignored in F-D4WM measurements (see text).

(B) one. In the backward set-up, the two pump beams are counter-propagating in the detection cell. A third (probe) beam intersects the other beams under a small angle, typically about 1°. In the forward set-up, all beams propagate in the same direction. It should be noted that in B-D4WM the pump beams interact over a large distance whereas in F-D4WM this distance is short (see Fig. 13).

In B-D4WM, E_f and E_p, the forward pump and probe beam, respectively, interfere at an angle $2\theta_{in}$, and the interference pattern induces an index grating from which beam E_b can diffract. From diffraction theory it is known that a grating diffracts an incoming beam according to:

$$\sin\theta_{out,k} = \frac{k\lambda}{2\Lambda} \tag{18}$$

where k is any integer. By taking θ_{in}as the value for θ in Eq. (17) and substituting this equation in Eq. (18), one obtains:

$$\sin\theta_{out,k} = \frac{k\lambda}{2\Lambda/2\sin\theta_{in}} = k\sin\theta_{in} \tag{19}$$

Because of the large interaction distance in B-D4WM, the Bragg condition is fully obeyed so that only $k=1$ is allowed. This implies that the signal beam, E_s, retraces the same path as E_p. It is separated from E_p by means of a beam splitter or by a polarization discrimination scheme [175].

In the forward configuration (Fig. 14), E_{p1} and E_{p2} intersect at an angle $2\theta_{in}$. As in the case of B-D4WM, the fringe distance of the induced grating can be calculated from Eq. (17). E_{p1} has an intensity of twice that of E_{p2}, since it also serves as the probe beam; E_{p1} is diffracted over more orders, corresponding to different values of k in Eq. (18). In F-D4WM, for $k=1$, part of E_{p1} is diffracted in E_{p2} and therefore will not be visible. Fortunately, because of the short interaction length, the grating thickness and Λ are of the same order of magnitude so that the Bragg condition is less strict and $k\neq1$ is not completely forbidden [176]. Under these circumstances a diffracted (signal) beam, E_s, will be visible which obeys the following equation:

$$\sin\theta_{out,n} = 2\sin\theta_{in} \tag{20}$$

Usually, the B-D4WM set-up is used in combination with long sample cells, i.e., with a large interaction length, which is advantageous for generating strong signals, since the Bragg condition is fulfilled. Conversely, in the F-D4WM set-up, emphasis is on the violation of the Bragg condition by using short cells. Furthermore, the signal generation efficiency is better in the F-D4WM set-up, since only two beams have to be aligned, and in B-D4WM more optics are required [177]. Hence, F-D4WM is the preferred mode in micro-separation systems: the set-up is much simpler and the requirement of a detection cell with a short optical pathlength is not a limitation. Therefore, in this section attention will be focused on F-D4WM.

The intensity of the F-D4WM signal beam, I_s, is given by [177,178]:

$$I_s = CI_1^2 I_2 \frac{\lambda^2}{\sin^2 2\theta_{in}} \cdot \left[\frac{\partial n}{\partial T}\right]^2 \cdot m^2(\varepsilon c l)^2 \cdot \frac{\eta^2}{\kappa^2} \tag{21}$$

where I_1 and I_2 are the beam powers of E_{p1} and E_{p2}, respectively; $\partial n/\partial T$ is the temperature gradient of the refractive index, κ the thermal conductivity of the solvent, m a ''mixing quality'' parameter (de-

pending on parameters such as overlap of the excitation beams, coherence length of the laser and the quality of the cell windows) and varies between 0 and 1; εcl is the absorbance of the Lambert–Beer equation. C is a proportionality constant and η the conversion efficiency for photon energy to heat contributing to the thermal grating, which can be expressed as [179]:

$$\eta = 1 - \phi_L \tag{22}$$

where ϕ_L is the luminescence quantum yield of the analyte. Eq. (22) shows that luminescence does not contribute to the thermal grating. Nonetheless, a further refinement of Eq. (22) is needed if fluorescent analytes are considered: even for molecules with a 100% quantum yield, heat is produced due to vibrational relaxation. Therefore, Eq. (22) should be extended to [179]:

$$\eta = 1 - \phi_L \cdot \frac{\lambda}{\lambda_{em}} \tag{23}$$

where λ_{em} is the wavelength of maximum fluorescence emission. Although fluorescence emission is broad-banded, it has been shown that Eq. (23) is a good approximation. The equation illustrates that LIF and F-D4WM are complementary techniques: when η suffers from a high value of ϕ_L, LIF should be the detection method of choice. On the other hand, for compounds showing no or hardly any native fluorescence, efficient D4WM signal generation can be expected [179].

Eq. (21) helps to understand some analytical characteristics of F-D4WM. In contrast to TLS, which also relies on laser light absorption, it is a zero-background technique: in the absence of analyte no E_s beam is generated [180]. As a result, the sensitivity of the technique depends almost exclusively on the collection efficiency of the signal which is, as was stated above, virtually 100% [177]. F-D4WM is a non-linear technique; the signal intensity is proportional to the square of the analyte concentration. The signal has a quadratic dependence on I_1, and a linear dependence on I_2, so that overall a cubic dependence on the laser power is obtained [177]. It can be derived from Eq. (21) that the optimal ratio I_1/I_2 is 2:1. It should be realized that, in addition to E_s, a second signal appears with an intensity that is half that of I_s. Since in practice only E_s is detected, the second beam will not be further considered here.

7.2. Instrumentation

Although pulsed lasers were used in the early stages of development of D4WM [181],, most publications deal with argon-ion lasers, which are usually operated in the visible range. The 351-nm line was studied only recently [182,183].

D4WM is, in principle, a zero-background technique but, in practice, one has to deal with the background at the same wavelength as the signal which is caused by reflection and refraction of laser light by the detector cell and the optics of the set-up. Special detector cell designs have been developed in order to reduce this scattering. A quartz detector cell with wedge-shaped windows was constructed to fulfil the Brewster condition both at the air–quartz and the quartz–liquid boundary so that reflections—for the air–quartz boundary as large as 4% and for the quartz–liquid boundary about 0.5%—are largely excluded (i.e, less than 0.01%) [180]. The internal volume of this cell was as large as 10 μl so that it can only be used in conventional-size LC. In microseparation systems square capillaries (with square inner and outer bores) are most promising [182]. Illumination under the air–quartz Brewster angle is still possible so that the largest contributing reflection to background scatter plays no role anymore.

Another approach to improve the signal-to-background ratio uses the fact that the signal beam is coherent (because it is a diffracted laser beam) whereas the background is not. If a scanning interferometer is used, which transmits the coherent signal beam but suppresses incoherent scatter light, an improvement of about 10^3 in terms of S/N is observed, which corresponds to a 30-fold improvement in terms of LODs [184]

Furthermore, a polarization discrimination scheme has been utilized. By using a circularly and a horizontally polarized pump beam, and detecting the vertically polarized component of the signal beam, scattering due to the horizontally polarized beam can be largely eliminated [185]. Here, the gain is 70-fold in terms of S/N.

Several attempts have been made to reduce the

size of the D4WM detection system. A diode laser has been used to design a very compact detector that can detect 7×10^{-5} absorbance units (AU) in a volume of only 160 pl [174]. Optical fibres have been applied in a design which, admittedly, still uses a large-size argon-ion laser. However, the rest of the optical system now requires less space since no alignment mirrors are needed anymore [186].

7.3. Coupling to separation systems

In flow systems, LODs in the attomole range have been obtained for D4WM by using laser-probed volumes of less than 100 pl [177]. This opens perspectives for D4WM as a detection technique in micro-separation systems, where conventional absorption detection is difficult to apply. However, in order to create optimum conditions, detection cells should have flat windows to provide a well-formed interference pattern and a proper flow-rate should be used, which is small enough to exclude adverse effects on the shape of the induced grating, but high enough to prevent photodecomposition. It has been shown that a flow of 0.5 μl min^{-1} (in commonly used 75-μm capillaries) is optimal for F-D4WM detection [182]. Finally, it will be imperative to use solvents with favourable $\partial n/\partial T$ and κ values. It is not easy to meet these conditions in actual practice. There is little freedom in flow-rate and solvent selection because both parameters are determined by the separation system used. Furthermore, detection cell construction should not adversely affect the separation power of the system.

The solvent parameters $\partial n/\partial T$ and κ have a distinct influence on the D4WM signal. To quote an example, when going from pure acetonitrile to pure water, the signal intensity will decrease 300-fold (Eq. (21) and Table 1). In practice, the situation may be more favourable. For example, in LC, with an organic modifier content of typically 50%, the D4WM signal will only be 6-fold lower [180]. On the other hand, in CE, aqueous buffers are usually applied without any organic modifier. It may, therefore, be expected that, in CE, the enhancement of D4WM over conventional absorption detection will be very small. It should be realized, however, that absorption detection itself is much less favourable in CE than in μLC since, in CE, Z- or U-shaped detection cells cannot be applied. Actually, an enhancement factor of 25 has been reported for CE–D4WM [183].

7.4. Practical usefulness

Table 6 summarizes literature data on the performance of various D4WM detection systems. Enhancement factors (versus conventional absorption detection) for LODs expressed in AU are included if these data were provided in the literature. Liquid-state D4WM is a novel technique, which helps to explain the limited number of publications. The first coupling of LC and D4WM was reported only 6 years ago and only two research groups are active in the field. The published papers deal only with standard solutions and have the objective to demonstrate the analytical performance of D4WM. Data on repeatability and linear dynamic range are never reported, and no real-life applications are shown.

Some general conclusions regarding D4WM can be drawn from Table 6. First, the forward mode is more frequently used in combination with LC and CE separations as opposed to FIA systems. As noted above, this mode is easier to implement while its performance is about the same as for the backward mode. Even if the data on conventional-size LC are not too convincing, one may say that the LODs, expressed in AU, are similar in conventional-size and μLC, viz. about 10^{-6} AU. This is in contrast with what is found in conventional absorption detection, where miniaturization frequently leads to a serious loss of performance as a result of shorter optical pathlengths and less light throughput [193]. Consequently, the enhancement of D4WM over absorption detection in μLC is considerable, with E values of 20–170.

Secondly, it has to be admitted that in all cited publications on LC–D4WM isocratic LC is used. Since a gradient will affect both κ and $\partial n/\partial T$, it will have a serious impact on signal generation during elution (cf. Eq. (21)) and, thus, on the robustness of F-D4WM detection. Obviously, such limitations do not hold for CE and isocratic LC.

Thirdly, the experimental results refer to the fixed wavelength provided by the laser, i.e., a wavelength that in general does not match the maximum of the absorption band of test analytes which generally is in

Table 6
Survey of literature data on D4WM detection coupled to separation systems

Analyte	D4WM mode	Laser type	Wavelength (nm)	(Average) power (mW)	LOD		*E*	Refs.
					(n*M*)	(μAU)		
Flow-injection analysis:								
Iodine	B	dye	540	1.5	80	600	–	[187]
Eosin B	B	Ar^+	488+514	1900	0.02	0	–	[188]
Co(II)	B	Ar^+	514	1000	30	3	–	[172]
Cd(II)	B	Ar^+	514	675	50 ng l^{-1}	2	–	[189]
Eosin B	F	Ar^+	514	500	7	2	–	[177]
Iodine	F	Ar^+	514	500	500	2	–	[177]
Rhodamine 800	F	diode	690	10	80	70	–	[174]
Co(III) (compl.)	F	Ar^+	514	250	30 000	–	–	[190]
Eosin B	F-FB[a]	Ar^+	514	240	1	1	–	[186]
Nitroaniline	F-FB[a]	Ar^+	514	100	700	50	–	[186]
Eosin B	F-FB[a]	Ar^+	514	50	80	100	–	[186]
Conventional-size LC:								
1-Aminoanthraquinone	F	Ar^+	514	800	600	20	~1	[180]
1-Aminoanthraquinone	F	Ar^+	514	800	20	0.5	30	[184]
Micro-bore LC:								
Amino acids (der.)	B	Ar^+	488	720	4000	–	–	[191]
1-Aminoanthraquinone	F	Ar^+	514	800	30	1	170	[179]
1-Aminoanthraquinone	F	Ar^+	514	1200	100	2	50	[192]
PAHs	F	Ar^+	351	500	30–60	4	20–70	[182]
2-Aminoanthraquinone	F	Ar^+	351	500	50	2	80	[182]
Capillary electrophoresis:								
Amino acids (der.)	F	Ar^+	458	30	2000	10	–	[185]
DNOC-based herbicides	F	Ar^+	351	500	1000	–	25	[183]

[a] F-FB, forward D4WM mode using optical fibres.

the deep UV. That is, as is also true for various other techniques discussed in this paper, D4WM will have only potential in analytical practice if lasers become available which provide sufficient power in the 200–250-nm region.

8. Conclusions and perspectives

When evaluating the state-of-the-art of the various laser-based detection techniques discussed above, it should be realized that there are at least three main problems. First, for almost all of the (sub-) techniques considered here, the number of published studies is relatively small and conclusions have, consequently, to be based on too few experimental data. Secondly, almost all reported data are based on the analysis of standard solutions—overall, there are less than 10 papers which deal with real-life samples. Thirdly, in several cases, the laser that should preferably be used for the technique being studied, either was not available or has been commercialized so recently that no convincing data have become available yet.

To complicate the issue, the merits of each of the detection techniques have to be evaluated for mutually rather different separation techniques, viz. conventional-size and μLC with their, often, high percentages of organic modifier and a general need for gradient elution conditions—and with, mutually, differences of flow-rates of about two orders of magnitude—versus CE with its essentially purely aqueous solution and a flow which is 10-fold smaller than even that of μLC. Nonetheless, conclusions based on the discussion presented above can be safely drawn. This can be facilitated by Table 7 in which the main characteristics of the various detection techniques discussed above are assembled.

Table 7
Evaluation and perspectives of the discussed detection technique

Detection technique	Laser(s) needed[a]	Aim[b]	Gain[c]	Aptness for microsystems[d]	Gradient compatible[e]	Aqueous solvent compatibility[f]	Universability[g]
Thermal lens spectroscopy	CW-UV~10 mW+ CW-VIS~1 mW	D	++	++	−	<	−
Photo acoustic detection	Pulsed (kHz) UV	D	+	−	−	<	−
Refr. index backscattering	CW-VIS~1 mW	D	···	++	−	>	+
Raman spectroscopy	CW/ML (100 MHz) UV–Vis	I	···	0	+	>	−
Four-wave mixing	CW-UV~100 mW	D	++	++	−	<	−

[a] ML, modelocked laser.
[b] D, detection; I, identification.
[c] (+) One order of magnitude over conventional UV absorption detection; (++) two orders of magnitude over conventional UV absorption detection; (···) comparison not applicable.
[d] (−) Serious hindrances exist; (+) measures needed (e.g., modifications of existing set-ups); (++) no special cells/measures needed.
[e] (−) Signals are gradient sensitive; (+) signals are gradient independent.
[f] (<) Disadvantageous; (>) advantageous (i.e., less noise or background).
[g] (−) Less universal (i.e., analytes should absorb light); (+) wide applicable (no chromophores needed).

When evaluating the RS data, it should be emphasized that the main objective of the technique is identification rather than detection. That is, limits of identification (LOI) based on spectral details are, in general, at least one decade less favourable than the LODs reported in Table 5. An additional disadvantage is that only a few papers published so far address the problem of identification and show Raman spectra. Obviously, this aspect will need much more attention in the future. Further, it should be realized that the most detailed spectral information is provided by conventional RS which is, at the same time, the least sensitive RS mode. In our view, it will only become applicable for conventional-size LC if special detector designs (as in the LCW approach) can be successfully combined with analyte-enrichment techniques. In μLC, implementation will be even more difficult.

At present, only one paper deals with deep-UV RRS combined with conventional-size LC. The LODs are impressive (15–50 $\mu g\ l^{-1}$ for PAHs) but it has to be admitted that analyte preconcentration is included in this outcome. The situation regarding the LOI, is not yet fully clear: RRS spectra provide less information than RS spectra. Whether or not the much more sensitive SER(R)S techniques will meet the analyst's demands in the detectability versus information trade-off, is—in our opinion—too early to say. The various published combinations with LC are not yet mature, and further progress with regard to technical and instrumental development may well cause a breakthrough.

As far as coupling with CE is concerned, the compatibility with microsystems is of major importance. Three techniques deserve a positive qualification here, TLS, RIBS and F-D4WM. Within this group, RIBS probably has the best perspectives: it is almost universally applicable, aqueous solutions as commonly used in CE do not cause serious signal reduction and, last but not least, simple and low-cost lasers can be used. In combination with analyte preconcentration techniques such as CIEF, concentration LODs of better than 1 μM have been reported. As regards chip-based separations, there are RIBS results from only one research group. Probably, in this case temperature stability does not as yet limit the LODs; that is, further developments can be expected in this field.

TLS has some perspective, especially in the pump-probe configuration. The real-life samples analysed by conventional LC showed a 100-fold enhancement compared with conventional absorption detection, but it should be added that the analytes were exceptionally well compatible with available laser line. In CE, enhancement in the 10–100 range is reported, and further exploratory work is recommended.

The state-of-the-art of F-D4WM detection shows that, to this date, argon-ion laser lines in the visible region and at 351 nm were used almost exclusively, and that virtually all work was done in the LC, not the CE area. Experiments in the deep-UV region, where most analytes have their maximum extinction coefficient, still have to be performed. Even though it is also true that only standard solutions were considered and gradient elution is known to cause problems, recently published data indicate that enhancement up to about 30-fold can be achieved due to the construction of a more sophisticated detection system which elegantly uses the coherence of the laser light. In μLC, enhancement is still better (*E*, 20–200) but, again, the absence of any information on experiments which come close to real-life situations/applications, should make us cautious. As regards CE, only one enhancement factor has been reported so far. Its satisfactory value of 25 (and the absence of gradient problems) may well indicate that F-D4WM will have a brighter future in this separation mode.

Finally, one might question whether novel laser systems will stimulate the practical implementation or change the future perspectives of the above techniques. Obviously, such an effect is absent in RI-based techniques, but this certainly applies for TLS and D4WM—which show future possibilities in CE—detection where the availability of tunable deep UV radiation is a prerequisite. For on-line LC–RS and CE–RS it is also very important: it will enable the recording of conventional RS and RRS spectra as a function of excitation wavelength. In the ideal situation this will be performed by means of a mode-locked laser (with a repetition rate as high as 100 MHz) to ensure significant sensitivity and a short pulses (typically a few ps) to be able to reduce or even exclude fluorescence background by means of time-gated detection. The laser systems needed to achieve this goal, such as Ti:sapphire laser systems, are expensive but rather robust and easy to operate.

References

[1] P.J.M. Kwakman, H. Koelewijn, I. Kool, U.A.Th. Brinkman, G.J. de Jong, J. Chromatogr. 511 (1990) 155.
[2] P.J.M. Kwakman, H.P. van Schaik, U.A.Th. Brinkman, G.J. de Jong, Analyst 116 (1991) 1385.
[3] A.J.G. Mank, E.J. Molenaar, H. Lingeman, C. Gooijer, U.A.Th. Brinkman, N.H. Velthorst, Anal. Chem. 65 (1993) 2197.
[4] A.J.G. Mank, H. Lingeman, C. Gooijer, J. High Resut. Chromatogr. Chromatogr. Commun. 11 (1994) 797.
[5] A.J.G. Mank, E.J. Molenaar, C. Gooijer, H. Lingeman, N.H. Velthorst, U.A.Th. Brinkman, J. Pharm. Biomed. Anal. 13 (1995) 255.
[6] A.J.G. Mank, H.T.C. van der Laan, H. Lingeman, C. Gooijer, U.A.Th. Brinkman, N.H. Velthorst, Anal. Chem. 67 (1995) 1742.
[7] A.J.G. Mank, E.S. Yeung, J. Chromatogr. A 708 (1995) 309.
[8] M.J. Nuijens, M. Zomer, A.J.G. Mank, C. Gooijer, N.H. Velthorst, J.W. Hofstraat, Anal. Chim. Acta 311 (1995) 47.
[9] A.J.G. Mank, M.C. Beekman, N.H. Velthorst, U.A.Th. Brinkman, C. Gooijer, Anal. Chim. Acta 315 (1995) 209.
[10] S.J. Kok, N.H. Velthorst, C. Gooijer, U.A.Th. Brinkman, Electrophoresis 19 (1998) 2753.
[11] T.H. Maiman, Nature 189 (1960) 493.
[12] T.H. Maiman, Br. Commun. Electron. 7 (1960) 794.
[13] T.H. Maiman, Phys. Rev. Lett. 4 (1960) 564.
[14] J.W. Robinson (Ed.), Handbook of Spectroscopy, CRC Press, Cleveland, OH, 1974.
[15] D.L. Andrews, in: Lasers in Chemistry, Springer, Berlin, 1990.
[16] A. Yariv, in: Optical Electronics, CBS College Publishing, New York, 1985, Chapter 8.
[17] R.J. van de Nesse, G.Ph. Hoornweg, C. Gooijer, U.A.Th. Brinkman, N.H. Velthorst, Anal. Chim. Acta 227 (1989) 173.
[18] K.C. Chan, G.M. Muschik, H.J. Issaq, Electrophoresis 21 (2000) 2062.
[19] K. Kuijt, C. García-Ruiz, G.J. Stroomberg, M.L. Marina, F. Ariese, U.A.Th. Brinkman, C. Gooijer, J. Chromatogr. A 907 (2001) 291.
[20] J. Wei, M.L. Gostkowski, M.J. Gordon, J.B. Shear, Anal. Chem. 70 (1998) 3740.
[21] J.B. Shear, Anal. Chem. 71 (1999) 598A.
[22] S.A. Asher, C.H. Munro, Z. Chi, Laser Focus World 33 (7) (1997) 99.
[23] C. Gooijer, A.J.G. Mank, Anal. Chim. Acta 400 (1999) 281.
[24] G.J. Blanchard, Appl. Spectrosc. 55 (2001) 110A.
[25] R.F. Service, Science 276 (1997) 895.
[26] http://www.nichia.co.jp
[27] A. Yariv, in: Optical Electronics, CBS College Publishing, New York, 1985, Chapter 6.
[28] A.J.G. Mank, H. Lingeman, C. Gooijer, Trends Anal. Chem. 11 (1992) 210.
[29] A.J.G. Mank, H. Lingeman, C. Gooijer, Trends Anal. Chem. 15 (1996) 1.
[30] R.D. Mead, C.I. Miyake, Laser Focus World 34 (1) (1998) 113.
[31] E.J. Lerner, Laser Focus World 34 (4) (1998) 91.

[32] E.J. Lerner, Laser Focus World 34 (2) (1998) 95.
[33] K. Niemax, A. Zybin, D. Eger, Anal. Chem. 73 (2001) 135A.
[34] J.E. Melanson, C.A. Lucy, Analyst 125 (2000) 1049.
[35] J.E. Melanson, C.A. Boulet, C.A. Lucy, Anal. Chem. 73 (2001) 1809.
[36] S.A. Ascher, R.W. Bormett, X.G. Chen, D.H. Lemmon, N. Cho, P. Peterson, M. Arrigoni, L. Spinelli, J. Cannon, Appl. Spectrosc. 47 (1993) 628.
[37] P.A. Harmon, J. Teraoka, S.A. Ascher, J. Am. Chem. Soc. 122 (1990) 8789.
[38] S.J. Kok, G.Ph. Hoornweg, T. de Ridder, U.A.Th. Brinkman, N.H. Velthorst, C. Gooijer, J. Chromatogr. A 806 (1998) 355.
[39] J.M. Harris, N.J. Dovichi, Anal. Chem. 52 (1980) 695A.
[40] J.P. Gordon, R.C.C. Leite, R.S. Moore, S.P.S. Porto, J.R. Whinnery, J. Appl. Phys. 36 (1965) 3.
[41] N.J. Dovichi, CRC Crit. Rev. Anal. Chem. 17 (1987) 357.
[42] G. Ramis-Ramos, Anal. Chim. Acta 283 (1993) 623.
[43] J.M. Saz, J.C. Díez-Masa, J. Liq. Chromatogr. 17 (1994) 499.
[44] R.D. Snook, R.D. Lowe, Analyst 120 (1995) 2051.
[45] Y. Martín-Biosca, M.C. García-Alvarez-Coque, G. Ramis-Ramos, Trends Anal. Chem. 16 (1997) 342.
[46] M. Franko, Talanta 54 (2001) 1.
[47] Y. Martín-Biosca, M.J. Medina-Hernández, M.C. García-Alvarez-Coque, G. Ramis-Ramos, Anal. Chim. Acta 296 (1994) 285.
[48] D. Beysens, P. Calmettes, J. Chem. Phys. 66 (1977) 766.
[49] G. Abbate, U. Bernini, F. Ragozzino, F. Somma, J. Phys. D 11 (1978) 1167.
[50] N.J. Dovichi, J.M. Harris, Anal. Chem. 51 (1979) 728.
[51] R.C. Weast (Ed.), CRC Handbook of Chemistry and Physics, 1st student ed., CRC Press, Boca Raton, FL, 1987.
[52] C.E. Buffett, M.D. Morris, Anal. Chem. 54 (1982) 1824.
[53] T.G. Nolan, B.K. Hart, N.J. Dovichi, Anal. Chem. 57 (1985) 2703.
[54] T.G. Nolan, D.J. Bornhop, N.J. Dovichi, J. Chromatogr. 384 (1987) 189.
[55] T.G. Nolan, N.J. Dovichi, Anal. Chem. 59 (1987) 2803.
[56] P.C.D. Hobbs, Optics and Photonics April (1991) 17.
[57] J. Zheng, T. Odake, T. Kitamori, T. Sawada, Anal. Sci. 15 (1999) 223.
[58] M. Harada, M. Shibata, T. Kitamori, T. Sawada, Anal. Sci. 15 (1999) 647.
[59] M. Tokeshi, M. Uchida, A. Hibara, T. Sawada, T. Kitamori, Anal. Chem. 73 (2001) 2112.
[60] Y.M. Biosca, J.J.B. Baeza, G. Ramis-Ramos, J. Pharm. Biomed. Anal. 41 (1996) 1037.
[61] Y.M. Biosca, J.J.B. Baeza, G. Ramis-Ramos, Chromatographia 44 (1997) 145.
[62] M. Šikovec, M. Novic, V. Hudnik, M. Franko, J. Chromatogr. A 739 (1996) 111.
[63] M. Šikovec, M. Franko, F.G. Cruz, S.A. Katz, Anal. Chim. Acta 330 (1996) 245.
[64] M.A. Proskurnin, N.V. Osipova, V.V. Kuznetsova, E.K. Ivanova, A.G. Abroskin, Analyst 121 (1996) 419.
[65] M.S. Baptista, C.D. Tran, Appl. Optics 36 (1997) 7059.
[66] R.A. Leach, J.M. Harris, J. Chromatogr. 218 (1981) 15.
[67] M. Xu, C.D. Tran, Anal. Chem. 62 (1990) 2467.
[68] A. Chartier, J. Georges, Anal. Chim. Acta 284 (1993) 311.
[69] C.D. Tran, G. Huang, V.I. Grishko, Anal. Chim. Acta 299 (1995) 361.
[70] E. Steinle, W. Faubel, H.J. Ache, Anal. Chim. Acta 353 (1997) 207.
[71] M. Franko, P. van den Bovenkamp, D. Bicanic, J. Chromatogr. B 718 (1998) 47.
[72] S. Luterotti, M. Sikovec, D. Bicanic, J. Pharm. Biomed. Anal. 21 (1999) 901.
[73] S. Luterotti, M. Sikovec, D. Bicanic, Talanta 53 (2000) 103.
[74] M. Šikovec, M. Novic, M. Franko, J. Chromatogr. A 706 (1995) 121.
[75] M. Šikovec, M. Franko, M. Novic, M. Veber, J. Chromatogr. A 920 (2001) 119.
[76] B. Divjak, M. Franko, M. Novic, J. Chromatogr. A 829 (1998) 167.
[77] K.J. Skogerboe, E.S. Yeung, Anal. Chem. 58 (1986) 1014.
[78] Z. Rosenzweig, E.S. Yeung, Appl. Spectrosc. 47 (1993) 8.
[79] M. Yu, N.J. Dovichi, Mikrochim. Acta III (1988) 27.
[80] M. Yu, N.J. Dovichi, Anal. Chem. 61 (1989) 37.
[81] K.C. Waldron, N.J. Dovichi, Anal. Chem. 64 (1992) 1396.
[82] J. Ren, B. Li, Y. Deng, J. Cheng, Talanta 42 (1995) 1891.
[83] B. Krattiger, A.E. Bruno, H.M. Widmer, R. Dändliker, Anal. Chem. 67 (1995) 124.
[84] K.C. Waldron, J. Li, J. Chromatogr. B 683 (1996) 47.
[85] B.S. Seibel, W. Faubel, J. Chromatogr. A 817 (1998) 223.
[86] M.J. Sepaniak, J.D. Vargo, C.M. Kettler, M.P. Maskarinec, Anal. Chem. 56 (1984) 1252.
[87] E.S. Yeung (Ed.), Detectors for Liquid Chromatography, Wiley, New York, 1986.
[88] D.S. Kliger (Ed.), Ultrasensitive Laser Spectroscopy, Academic Press, New York, 1983.
[89] P. Hess, J. Pelzl (Eds.), Photoacoustic and Photothermal Phenomena, Springer, New York, 1987.
[90] Y. Kohanzadeh, J.R. Whinnery, M.M. Carroll, J. Acoust. Soc. Am. 57 (1975) 67.
[91] C.K.N. Patel, A.C. Tam, Rev. Mod. Phys. 53 (1981) 517.
[92] W. Schrepp, R. Stumpe, J.I. Kim, H. Walther, Appl. Phys. B 32 (1983) 207.
[93] J. Wu, T. Kitamori, T. Sawada, Anal. Chem. 62 (1990) 1676.
[94] J. Wu, T. Odake, T. Kitamori, T. Sawada, Anal. Chem. 63 (1991) 2216.
[95] T. Odake, T. Kitamori, T. Sawada, Anal. Chem. 69 (1997) 2537.
[96] R.E. Synovec, Anal. Chem. 59 (1987) 2877.
[97] E.P.C. Lai, S.Y. Su, E. Voigtman, J.D. Winefordner, Chromatographia 15 (1982) 645.
[98] W. Lahman, H.J. Ludewig, H. Welling, Anal. Chem. 49 (1977) 549.
[99] S. Oda, T. Sawada, H. Kamada, Anal. Chem. 50 (1978) 865.
[100] V.P. Zharov, V.S. Lethokov, in: Laser Optoacoustic Spectroscopy, Springer, Heidelberg, 1986, Chapter 9.
[101] E. Voigtman, A. Jurgensen, J. Winefordner, Anal. Chem. 53 (1981) 1443.
[102] P. Hodgson, K.M. Quan, H.A. MacKenzie, S.S. Freeborn, J. Hannigan, E.M. Johnson, F. Greig, T.D. Binnie, Sensors Actuators B 29 (1995) 339.

[103] T. Autrey, N. Foster, D. Hopkins, J. Price, Anal. Chim. Acta 434 (2001) 217.
[104] R. Stumpe, J.I. Kim, W. Schrepp, H. Walther, Appl. Phys. B 34 (1984) 203.
[105] T. Odake, T. Kitamori, T. Sawada, Anal. Chem. 64 (1992) 2870.
[106] I. Carrer, P. Cusmai, E. Zanzottera, W. Martinotti, F. Realini, Anal. Chim. Acta 308 (1995) 20.
[107] S. Oda, T. Sawada, Anal. Chem. 53 (1981) 471.
[108] T. Odake, T. Kitamori, T. Sawada, Anal. Chem. 67 (1995) 145.
[109] S.Z. Lewin, N. Bauer, in: I.M. Kolthoff, P.J. Elving (Eds.), Treatise on Analytical Chemistry, Part I, Vol. 6, Wiley-Interscience, New York, 1965, Chapter 70.
[110] J.D. Jackson, Classical Electrodynamics, 2nd ed., New York, 1975, Chapter 4.
[111] A.E. Bruno, B. Krattiger, F. Maystre, H.M. Widmer, Anal. Chem. 63 (1991) 2689.
[112] D.J. Bornhop, N.J. Dovichi, Anal. Chem. 59 (1987) 1632.
[113] D.J. Bornhop, T.G. Nolan, N.J. Dovichi, J. Chromatogr. 384 (1987) 181.
[114] B. Krattiger, G.J.M. Bruin, A.E. Bruno, Anal. Chem. 66 (1994) 1.
[115] K. Swinney, D. Markov, D.J. Bornhop, Anal. Chem. 72 (2000) 2690.
[116] A.J.G. Mank, O. Larsen, H. Lingeman, C. Gooijer, U.A.Th. Brinkman, N.H. Velthorst, Anal. Chim. Acta 323 (1996) 1.
[117] D.J. Bornhop, Appl. Opt. 34 (1995) 3234.
[118] H.J. Taragan, P. Neill, C.K. Kenmore, D.J. Bornhop, Anal. Chem. 68 (1996) 1762.
[119] J. Wu, J. Pawliszyn, Anal. Chem. 64 (1992) 2934.
[120] J. Wu, J. Pawliszyn, Anal. Chem. 66 (1994) 867.
[121] K. Swinney, D.J. Bornhop, J. Microcol. Sep. 11 (1999) 696.
[122] K. Swinney, J. Pennington, D.J. Bornhop, Analyst 124 (1999) 221.
[123] K. Swinney, D. Markov, J. Hankins, D.J. Bornhop, Anal. Chim. Acta 400 (1999) 265.
[124] Y. Deng, B. Li, Appl. Opt. 37 (1998) 1001.
[125] J. Pawliszyn, Anal. Chem. 60 (1988) 2796.
[126] J. Wu, J. Pawliszyn, Anal. Chem. 64 (1992) 219.
[127] A. Lyon, C.D. Keating, A.P. Fox, B.E. Baker, L. He, S.R. Nicewarner, D.P. Mulvaney, S.R. Nathan, Anal. Chem. 70 (1998) 341R.
[128] D.A. Skoog, J.J. Leary, in: Principles of Instrumental Analysis, 4nd ed., Saunders College Publishing, Orlando, FL, 1992, Chapter 13.
[129] S.A. Asher, Anal. Chem. 65 (1993) 201A.
[130] C.L. Stevenson, T. Vo-Dinhin, in: J.J. Laserna (Ed.), Modern Techniques in Raman Spectroscopy, Wiley, Chichester, 1996, Chapter 1.
[131] D.L. Jeanmaire, R.P. van Duyne, J. Electroanal. Chem. 84 (1977) 1.
[132] K. Kneipp, H. Kneipp, I. Itzkan, R.R. Dasari, M.S. Feld, Chem. Rev. 99 (1999) 2957.
[133] S. Nie, S.R. Emory, Science 275 (1997) 1102.
[134] J.A. Pezzuti, M.D. Morris, Anal. Comm. 34 (1997) 5H.
[135] S.A. Asher, Anal. Chem. 65 (1993) 59A.
[136] R.J. Dijkstra, C.T. Martha, F. Ariese, U.A.Th. Brinkman, C. Gooijer, Anal. Chem. 73 (2001) 4977.
[137] P.A. Walker III, W.K. Kowalchyk, M.D. Morris, Anal. Chem. 67 (1995) 4255.
[138] P.A. Walker III, M.D. Morris, J. Chromatogr. A 805 (1998) 269.
[139] P.A. Walker III, M.D. Morris, M.A. Burns, B.N. Johnson, Anal. Chem. 70 (1998) 3766.
[140] R.J. Dijkstra, A.N. Bader, G.Ph. Hoornweg, U.A.Th. Brinkman, C. Gooijer, Anal. Chem. 71 (1999) 4575.
[141] R.J. Dijkstra, C.J. Slooten, A. Stortelder, J.B. Buijs, F. Ariese, U.A.Th. Brinkman, C. Gooijer, J. Chromatogr. A 918 (1999) 25.
[142] G.W. Somsen, S.K. Coulter, C. Gooijer, N.H. Velthorst, U.A.Th. Brinkman, Anal. Chim. Acta 349 (1997) 189.
[143] R.M. Seifar, R.J. Dijkstra, U.A.Th. Brinkman, C. Gooijer, Anal. Commun. 36 (1999) 273.
[144] R.M. Seifar, M.A.F. Altelaar, R.J. Dijkstra, F. Ariese, U.A.Th. Brinkman, C. Gooijer, Anal. Chem. 72 (2000) 5718.
[145] B.J. Marquardt, P.G. Vahey, R.E. Synovec, L.W. Burgess, Anal. Chem. 71 (1999) 4808.
[146] T.D. Nguyen Hong, M. Jouan, N.Q. Dao, M. Bouraly, F. Mantisi, J. Chromatogr. A 743 (1996) 323.
[147] R. Steinert, H. Bettermann, K. Kleinermanns, Appl. Spectrosc. 51 (1997) 1644.
[148] B.J. Marquardt, K.P. Turney, L.W. Burgess, Proc. Soc. Photo-Opt. Instrum. 3860 (1999) 239.
[149] M. D'Orazio, U. Schimpf, Anal. Chem. 53 (1981) 809.
[150] N.J. Pothier, R.K. Forcé, Appl. Spectrosc. 48 (1994) 421.
[151] S.A. Soper, K.L. Ratzlaff, T. Kuwana, Anal. Chem. 62 (1990) 1438.
[152] L.M. Cabelín, A. Rupérez, J.J. Laserna, Anal. Chim. Acta 318 (1996) 203.
[153] F. Ni, L. Thomas, T.M. Cotton, Anal. Chem. 61 (1989) 888.
[154] S.D. Cooper, M.M. Robson, D.N. Batchelder, K.D. Bartle, Chromatographia 44 (1997) 257.
[155] H. Koizumind, Y. Suzuki, J. High Resolut. Chromatogr. Chromatogr. Commun. 10 (1987) 173.
[156] C.-Y. Chen, M.D. Morris, J. Chromatogr. 540 (1991) 355.
[157] W.K. Kowalchyk, P.A. Walker III, M.D. Morris, Appl. Spectrosc. 49 (1999) 1183.
[158] L. He, M.J. Natan, C.D. Keating, Anal. Chem. 72 (2000) 5348.
[159] G.L. Devault, M.J. Sepaniak, Electrophoresis 22 (2001) 2303.
[160] W.F. Nirode, G.L. Devault, M.J. Sepaniak, R.O. Cole, Anal. Chem. 72 (2000) 1866.
[161] C.-Y. Chen, M.D. Morris, Appl. Spectrosc. 42 (1988) 515.
[162] P.A. Walker III, J.M. Shaver, M.D. Morris, Appl. Spectrosc. 51 (1997) 1394.
[163] R.L. Farrow, D.J. Rakestraw, Science 257 (1992) 1894.
[164] R.A. Fisher (Ed.), Optical Phase Conjugation, Academic Press, New York, 1983.
[165] D.S. Moore, S.C. Schmidt, J.W. Shaner, Phys. Rev. Lett. 50 (1983) 1819.

[166] J. Pender, L. Hesselink, Opt. Lett. 10 (1985) 264.
[167] G. Hall, B.J. Whitaker, J. Chem. Soc. Faraday Trans. 90 (1994) 1.
[168] I.C. Khoo, P.Y. Yan, G.M. Finn, T.H. Liu, R.R. Michael, J. Opt. Soc. B 5 (1988) 202.
[169] R.K. Jain, R.C. Lind, J. Opt. Soc. Am. 73 (1983) 647.
[170] H. Fujiwara, K. Nakagawa, Opt. Commun. 55 (1985) 386.
[171] A.P. Smith, A.G. Astill, Appl. Phys. B 58 (1994) 459.
[172] Z. Wu, W.G. Tong, Anal. Chem. 63 (1991) 1943.
[173] H.J. Hoffman, IEEE J. Quant. Electron. QE-22 (1986) 552.
[174] S. Berniolles, Z. Wu, W.G. Tong, Spectrochim. Acta 49B (1994) 1473.
[175] A. Yariv, D.M. Pepper, Opt. Lett. 1 (1977) 16.
[176] C.V. Heer, N.C. Griffen, Opt. Lett. 4 (1979) 239.
[177] Z. Wu, W.G. Tong, Anal. Chem. 65 (1993) 112.
[178] F. Simoni, G. Cipparone, D. Duca, I.C. Khoo, Opt. Lett. 16 (1991) 360.
[179] T. de Beer, G.Ph. Hoornweg, A. Termaten, U.A.Th. Brinkman, N.H. Velthorst, C. Gooijer, J. Chromatogr. A 811 (1998) 35.
[180] T. de Beer, G.Ph. Hoornweg, G.J. Grootendorst, N.H. Velthorst, C. Gooijer, Anal. Chim. Acta 330 (1996) 189.
[181] J.M. Ramsey, W.B. Whitten, Anal. Chem. 59 (1987) 167.
[182] T. de Beer, G.Ph. Hoornweg, P. Besoo, U.A.Th. Brinkman, N.H. Velthorst, C. Gooijer, Appl. Spectrosc. 53 (1999) 595.
[183] T. de Beer, G.Ph. Hoornweg, F. Ariese, N.H. Velthorst, U.A.Th. Brinkman, C. Gooijer, Anal. Chim. Acta 416 (2000) 151.
[184] G.Ph. Hoornweg, T. de Beer, N.H. Velthorst, C. Gooijer, Appl. Spectrosc. 51 (1997) 1008.
[185] Z. Wu, W.G. Tong, J. Chromatogr. A 773 (1997) 291.
[186] J.A. Nunes, W.G. Tong, Appl. Spectrosc. 52 (1998) 763.
[187] K. Fujiwara, K. Kurokawa, H. Uchiki, T. Kobayashi, Spectrosc. Lett. 20 (1987) 633.
[188] Z. Wu, W.G. Tong, Anal. Chem. 61 (1989) 998.
[189] Z. Wu, J. Liu, W.G. Tong, Spectrochim. Acta 49B (1994) 1483.
[190] J.A. Nunes, W.G. Tong, Anal. Chem. 65 (1993) 2990.
[191] Z. Wu, W.G. Tong, J. Chromatogr. A 805 (1998) 63.
[192] T. de Beer, P. Besoo, G.Ph. Hoornweg, N.H. Velthorst, U.A.Th. Brinkman, C. Gooijer, Anal. Chim. Acta 390 (1999) 55.
[193] A.A. Abbas, D.C. Shelly, J. Chromatogr. A 691 (1995) 37.